Volume 19 | Number 22 | 21 November 2017 | Pages 5259–5516

Green Chemistry

Cutting-edge research for a greener sustainable future

rsc.li/greenchem

ISSN 1463-9262

ROYAL SOCIETY OF CHEMISTRY

CRITICAL REVIEW

An Verberckmoes *et al.*

Recent advances on the utilization of layered double hydroxides (LDHs) and related heterogeneous catalysts in a lignocellulosic-feedstock biorefinery scheme

Green Chemistry

CRITICAL REVIEW

Cite this: *Green Chem.*, 2017, **19**, 5269

Recent advances on the utilization of layered double hydroxides (LDHs) and related heterogeneous catalysts in a lignocellulosic-feedstock biorefinery scheme

Willinton Y. Hernández,[a] Jeroen Lauwaert,[b] Pascal Van Der Voort[a] and An Verberckmoes*[b]

Received 14th September 2017,
Accepted 4th October 2017

DOI: 10.1039/c7gc02795h

rsc.li/greenchem

Layered double hydroxides (LDHs) and derived materials have been widely used as heterogeneous catalysts for different types of reactions either in gas or in liquid phase. Among these processes, the valorization/upgrading of lignocellulosic biomass and derived molecules have attracted enormous attention because it constitutes a pivotal axis in the transition from an economic model based on fossil resources to one based on renewable biomass resources with preference for biomass waste streams. Proof of this is the increasing amount of literature reports regarding the rational design and implementation of LDHs and related materials in catalytic processes such as: depolymerization, hydrogenation, selective oxidations, and C–C coupling reactions, among others, where biomass-derived compounds are used. The major aim of this contribution is to situate the most recent advances on the implementation of these types of catalysts into a lignocellulosic-feedstock biorefinery scheme, highlighting the versatility of LDHs and derived materials as multifunctional, tunable, cheap and easy to produce heterogeneous catalysts.

1. Introduction

During the past few years, the biorefinery concept has emerged as a promising alternative where the sustainable processing of biomass instead of petroleum can be used for the production of bio-fuels and high-added value chemicals.[1–3] In this concept, the use of non-food waste biomass (second generation feedstock) is extremely important in order to avoid competition with food resources and to fit the 12 principles of Green Chemistry, more specifically, the principle related to the efficient utilization of raw materials, such as the waste produced from the agricultural sector.[4] Lignocellulosic feedstock (*e.g.* hard and soft wood, wheat straw, switchgrass, *etc.*) is the most abundant and cheapest inedible biomass source and therefore, it has been identified as a scalable and economically viable bio-source for the sustainable production of chemicals and fuels.[3,5] Lignocellulosic biomass is composed of three major biopolymers: cellulose, hemicellulose and lignin, which are insoluble polymers of glucose, related sugars such as xylose, and phenyl propane derivatives, respectively (Fig. 1).

The pretreatment of the lignocellulosic feedstock is a crucial step in an integrated biorefinery process in order to disintegrate and fractionate the three main components of the biomass source and, subsequently, be able to perform the conversion/upgrading of the derived chemical compounds. Many pretreatment processes have been proposed and reviewed, including physical (mechanical comminution), physicochemical (steam explosion, hydrothermolysis, and ammonia fiber explosion (AFEX)), chemical (lime and diluted acid), thermochemical (gasification and fast pyrolysis) and the combination of the aforementioned methodologies.[7–10] The selection of a specific pretreatment method mainly depends on the nature and chemical composition of the biomass source, cost involved and the degree of recovery/valorization of the obtained fractions. Later on, an efficient implementation of the integrated biorefinery concept should involve the development of chemical and/or catalytic routes to valorize all the obtained fractions (*i.e.* cellulose, hemicellulose and lignin), going from the production of the so-called platform molecules (*e.g.* furfural, hydroxymethyl furfural, levulinic acid, *etc.*) to the upgrading of these platform molecules to higher added-value products.

This condition has triggered enormous research efforts on the creation of new catalytic processes and catalysts (character-

[a]*Center for Ordered Materials, Organometallics & Catalysis (COMOC), Department of Inorganic and Physical Chemistry, Ghent University, Krijgslaan 281-S3, 9000 Ghent, Belgium*
[b]*Industrial Catalysis and Adsorption Technology (INCAT), Department of Materials, Textiles and Chemical Engineering (MaTCh), Ghent University, Valentin Vaerwyckweg 1, 9000 Ghent, Belgium. E-mail: An.Verberckmoes@UGent.be*

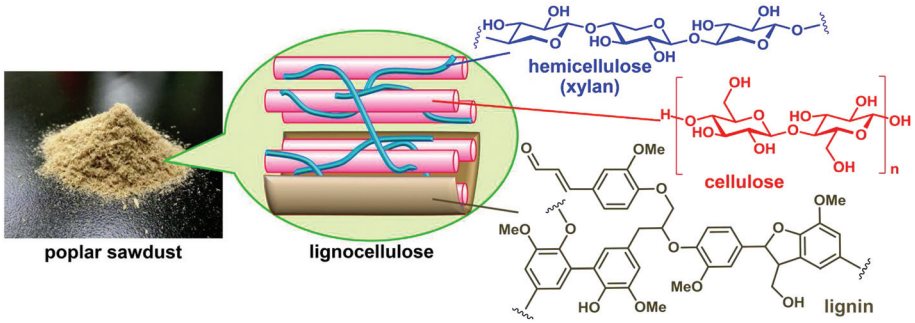

Fig. 1 Structure of lignocellulosic biomass. Reproduced from ref. 6 with permission from The Royal Society of Chemistry.

ized by multifunctional properties and robustness) in order to produce economically viable lignocellulosic-derived fuels and chemicals. In this context, the scientific knowledge inherited from the fossil-fuel based refineries has been extremely important as the catalytic systems established for the transformation/upgrading of oil-petrol, coal, shale gas and its derivatives can be potentially implemented in the different reaction steps involved in the biorefinery process. Despite the enormous amount of catalysts (heterogeneous and homogeneous) developed for the refining and petrochemical industries, three main families of materials have been widely studied and implemented due to their versatility in composition, production cost, robustness and multifunctional properties: (i) inorganic metal oxides, (ii) zeolites, and (iii) layered double hydroxides (LDHs) and derived materials.[11–14] These types of heterogeneous catalysts are already playing a relevant role in several biomass valorization processes (including lignocellulosic biomass), as can be seen from the numerous scientific reports and literature revisions dedicated to this topic.[15–23] Nonetheless, most of the reviews currently available in the literature are focused on the utilization and potential of inorganic metal oxides (either pure or mixed metal oxides) and zeolites for biomass transformation (and derived platform molecules), and less attention has been given to LDH-type and derived catalysts.

2. Focus of the review

The aim of this paper is to revise and critically assess the most relevant literature reports related to the utilization of LDHs and derived catalysts in the transformation of lignocellulosic biomass considering both the role played by these catalysts in the depolymerization-fractioning of the lignocellulosic-derived biopolymers, and the upgrading of the major platform molecules obtained from them (as schematized in Fig. 2).

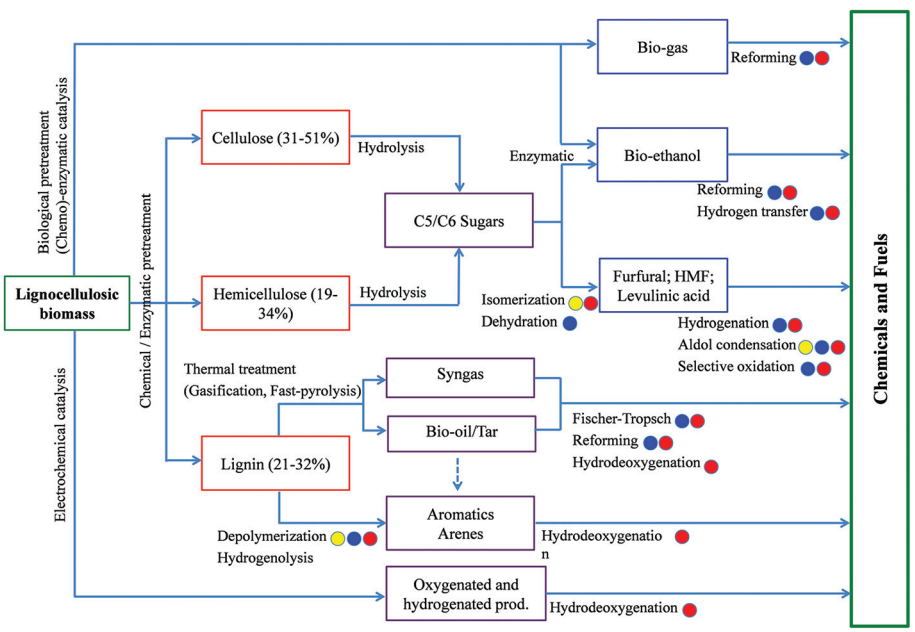

Fig. 2 Schematic representation on the role played by LDHs and derived catalysts in a lignocellulosic bio-refinery process (yellow: basic catalysts; blue: metal-supported catalysts; red: multifunctional catalysts).

Fig. 2 describes some of the most representative compounds (precursors, platform molecules and building block units) and transformation routes (mainly chemical) that could be considered in a biorefinery process involving a lignocellulosic feedstock. In addition, we have situated the participation of LDHs and derived materials as heterogeneous catalysts (as a function of their functionality indicated in different colors) in the described chemical reactions, which highlights the role played by these materials in an integrated biorefinery concept.

First, this review gives a general overview of the structure-to-functionality properties of LDHs and derived catalysts, taking into account the key features that make these materials suitable and promising catalytic systems for the valorization of lignocellulosic-biomass. Secondly, the conversion of cellulose and hemicelullose derivatives into C5/C6 sugars and the upgrading of platform molecules (furfural, hydroxymethyl furfural, levulinic acid and bio-ethanol) with the intervention of LDHs are discussed (see Fig. 2). Then, the conversion with LDHs and derived catalysts of lignin and lignin-derivatives into platform molecules (such as syngas and bio-oil) is given.

Although this literature revision is focused on the design and utilization of LDHs and derived materials as catalysts for a lignocellulosic biorefinery scheme, we have included additional information (presented in tables) comparing the catalytic performance of these materials with other reference catalysts. Relevant reference systems were chosen as a function of their metal composition in order to be compared with the reviewed LDHs and derived catalysts.

The advantages and/or challenges of LDH-derived catalysts against other heterogeneous catalytic systems were highlighted considering the "green" aspects of the discussed reactions.

Finally, the main conclusions, challenges and future perspectives are provided.

3. Structure-to-functionality properties of LDHs and derived catalysts

Layered double hydroxides (LDHs) or hydrotalcite-like compounds are a well-known family of anionic clay materials consisting of positively charged two-dimensional sheets (brucite-type structure), which have intercalated water and exchangeable charge-compensation anions (such as OH^-, CO_3^{2-}, NO_3^-, *etc.*). The lamellar structure is composed of octahedrons formed by sharing their edges with divalent and trivalent metal cations in the center and six hydroxide ions at the vertices[24–26] (Fig. 3).

Although the relationship between the structural and catalytic properties of these types of materials has been widely covered in several literature revisions,[11,20,24,27–30] this section highlights the importance of the LDH structure for the design of highly active and stable heterogeneous catalysts to be implemented in a biorefinery process.

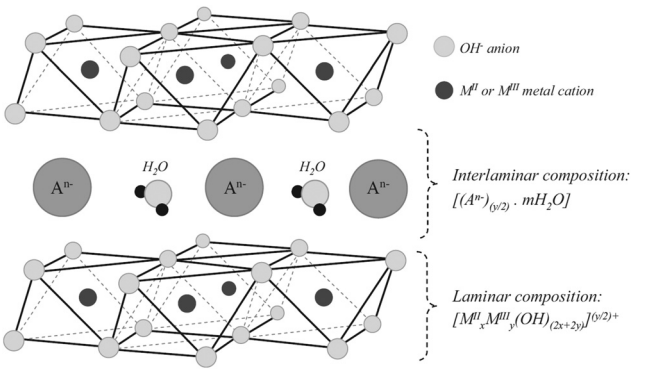

Fig. 3 Schematic representation of the layered double hydroxide structure. Reproduced from ref. 31 with permission from Elsevier.

In a recent literature revision, Li *et al.*[20] summarized several advantages of the utilization of LDHs in the field of heterogeneous catalysis. From those advantages, we have selected three properties as the most relevant ones for the design of solid catalysts for biorefinery processes: (i) cation-tunability of the brucite-like layers and anionic exchangeability, which provides to the LDHs-derived catalysts a wide versatility in composition;[26,32] (ii) tunable basicity of the surface in both, nature (Brønsted and Lewis type basic sites) and strength (from weak–middle to strong basic sites);[28,33] and (iii) uniform dispersion of M^{2+} and M^{3+} cations in the layers, as well as preferred orientation of anions in the interlayer, allowing the formation of highly dispersed and stable metal supported catalysts.[34] In addition, as all the previously mentioned properties can coexist in a single solid catalyst, the multifunctionality can be seen as an intrinsic characteristic of this family of materials.

3.1 Solid-base catalysts

One of the most relevant properties of LDHs and derived mixed metal oxides (MMO) is that they behave as solid bases. For this reason, these types of materials have been widely explored as heterogeneous catalysts for different base-catalyzed organic reactions, such as aldol condensation, transesterification, and alkylation, among others.[11] The Mg–Al hydrotalcites (HTs) and their calcination products have been reported as one of the most important and versatile group of basic catalysts derived from an LDH structure.[11,28,30]

The origin of the basic properties of these materials is directly related to their structure, chemical composition and thermal activation conditions. As was mentioned before, the structure of the LDH is characterized by the presence of structural OH^- groups (Fig. 3), which can be seen as Brønsted-type basic sites by themselves. Additionally, by favoring the presence of these hydroxyl groups as charge-compensation anions, the concentration and availability of the Brønsted-type basic sites of the catalyst can be strongly improved.

One of the most successful ways to increase the concentration and accessibility of the OH^- species at the interlayer space of the LDH structure is *via* the "reconstruction"

approach. This methodology takes advantage of the memory effect characteristic of calcined hydrotalcites (*i.e.* the derived mixed metal oxides) when they are thermally activated at a temperature below 550 °C. Thus, by putting the calcined material in contact with water vapor or liquid decarbonated water under inert atmosphere, the layered structure can be reconstructed by a retro-topotactical transformation, and mainly OH^- anions will remain at the interlayer gallery as compensating ions[35–37] (see Fig. 4). In addition, when the reconstruction is performed in liquid-phase and assisted by ultrasound, the breaking down of the crystal domain size favors an increase in the surface area of the material and accessibility to the intercalated hydroxyl groups.[38,39]

Recently, Takehira highlighted the influence of the rehydration of calcined LDHs on different types of reactions, such as aldol condensation, epoxidation, glycerol carbonate synthesis, and isomerization, among others.[40] Although these types of catalysts can be seen as an alternative to conventional inorganic bases (*e.g.* NaOH and KOH) in the fine chemical industry, technical barriers related to the fast poisoning of the OH^- centers in contact with air, low catalyst reusability and time-consuming regeneration steps, place reconstructed LDHs still far away from an industrial-scale application.

On the other hand, when a different type of basic site and/or high-thermally stable catalyst is required, the calcination of the LDH structure at intermediate temperatures (450–600 °C) provokes the formation of an MMO-type material with large surface area and high concentration of strong Lewis basic and mild Lewis acid sites.[41,42] Those types of acid-basic sites are associated with the creation of O^{2-}–M^{n+} acid–base pairs, where the Lewis basicity is related to the presence of low-coordination O^{2-} species in close interaction with M^{2+} cations (*e.g.* Mg^{2+}), and the Lewis acidity is due to the M^{3+} cations (*e.g.* Al^{3+}).

The strength and nature of the acidic–basic sites of these types of catalysts can be tailored by playing with four main parameters: (i) the nature of the substituting cations in the LDH structure; (ii) the characteristic M^{2+}/M^{3+} molar ratio (typically, the Mg/Al ratio in hydrotalcites and derived materials); (iii) the nature of the anions in the interlayer region; and (iv) the thermal activation performed on the layered materials (higher calcination temperatures favor the formation of Lewis basic sites).[26,28,30] For instance, in a very complete study, Valente *et al.*[43] reported the influence of different metal cations (M^{2+} = Mg^{2+}, Ni^{2+}, Zn^{2+}/M^{3+} = Al^{3+}, Fe^{3+}, Cr^{3+}) on the basic properties of MMO derived from LDH structures. These authors found that the basicity of the calcined materials is influenced by the differences of electronegativity between the studied cations, which affect the partial charge of the surface O^{2-} species. Other reports showed that the presence of less basic cations than Mg^{2+}, such as Zn^{2+} or Ni^{2+}, decreases the basic strength of both LDH and MMO type catalysts,[44–46] being able to modify the acid–base properties of the materials just by partial or total substitution of the M^{2+} cationic species.

Next to this, the number of basic sites and their strength can be also controlled by fine-tuning the M^{2+}/M^{3+} molar ratio.[47–51] In general, in the case of Mg–Al hydrotalcites, an increase in the amount of Al^{3+} causes a decrease in the total number of basic sites; however, the proportion of strong basic sites is augmented. In this manner, the selection of the best composition for LDHs and derived catalysts would depend on the reaction requirements in terms of density, strength and nature of the acid and basic sites, as a way to favor the efficiency of the catalytic reaction towards the desired product.

A general description of different characterization techniques used to evaluate the basic properties of LDH materials was previously disclosed by Debecker *et al.*[28] The combination of acidic probe molecules, such as CO_2, and different physicochemical characterization techniques (*e.g.* IR spectroscopy, temperature programmed desorption, calorimetric measurements, isotopic exchanges and thermogravimetric analysis) can be used to determine the nature, strength and concentration of the surface basic sites. For instance, the reactive adsorption of CO_2 on basic sites provokes the formation of different types of carbonate species whose nature (unidentate carbonate, bidentate carbonate and bicarbonate) and thermal stability can be directly related to the type (Brønsted or Lewis) and strength of the adsorption sites. These types of carbonate species can be studied by IR analysis in the dynamic ("*in situ*") mode.

In addition, the total amount of basic sites can be established *via* the CO_2 temperature-programmed desorption technique (CO_2-TPD), by measuring the volume of CO_2 released from the material surface (previously pretreated to adsorb CO_2 at a given temperature) and as a function of temperature. The temperature interval at which the CO_2 release happens during the CO_2-TPD analysis is proportional to the strength of the basic sites involved as well as their density.

Additional examples on calorimetry measurements, adsorption of different acidic molecules such as SO_2, trimethyl borate

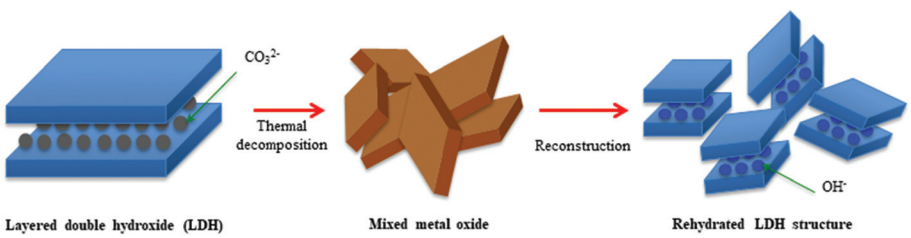

Fig. 4 Activation of Mg–Al hydrotalcite by thermal decomposition followed by reconstruction.

and CH_3CN, as well as titration techniques using different organic acids (*e.g.* benzoic acid, acrylic acid, *etc.*) to characterize the basic properties of LDHs can be seen in detail in ref. 28.

3.2 Metal-supported catalysts

The synthesis of highly dispersed and stable metal-supported nanoparticles (NPs) has been a major challenge in the design of efficient and robust heterogeneous catalysts. In general, these types of supported catalysts are prepared by "classic" deposition–precipitation and incipient wetness impregnation methods. However, in many cases, the supported NPs are inhomogeneously distributed and the weak metal-support interactions generated can lead to the migration and aggregation of the NPs either during the thermal activation-pretreatment of the catalyst or during the catalytic reaction.[30]

LDH-type structures have been used as active (functional) catalytic supports for the "classic" deposition of different types of NPs (*e.g.* Au, Ni, Ru, Pd).[20] Additionally, the uniform distribution of the M^{2+} and M^{3+} cations in the layered structure makes these materials excellent precursors for the preparation of highly dispersed metal-supported catalysts.[52–57] This preparation approach requires the introduction of the catalytically active species as substituted cations in the structure of the LDHs during the synthesis, followed by calcination and reduction steps. It allows the formation of well-dispersed metal NPs on a mixed oxide matrix (MMO).

This preparation methodology has been widely used for the preparation of transition metal (NPs) supported catalysts, Ni, Cu and Pd being the most common monometallic reported systems.[58–64] Additionally, by introducing two different reducible cations in the LDH structure (*e.g.* Ni–Cu;[65–67] Ni–Co,[68–70] Pd–Cu,[71,72] among others), the subsequent thermal activation/reduction can lead to the formation of bimetallic catalysts, whose catalytic and stability properties are generally better than those of the respective monometallic systems.

The anion-exchange capacity of LDHs has also been exploited as a way to incorporate well-dispersed catalytic species in the interlayer-gallery space.[73–75] This methodology requires the utilization of inorganic anions or anionic organometallic complexes, whose exchange capacity will depend on several factors, such as the charge density of the host layers (which depends on the M^{2+}/M^{3+} molar ratio) and the dynamic radius of the complex anion. Moreover, the electrostatic interactions between LDH layers and catalytically active anions can induce an ordered arrangement of interlayer species and tailor the orientation of the active sites.[30,76]

These two methodologies used to introduce reducible cations (mainly divalent transition metals) into the structure of LDHs are schematized in Fig. 5, where the preparation of the targeted metal-supported catalyst would require the additional reduction step of the desired catalytic species either by chemical or by thermal treatments.

An interesting feature reported for this type of metal supported catalysts is the synergistic interaction that may take place when combining an M^{II}–Mg–Al LDH-derived catalyst

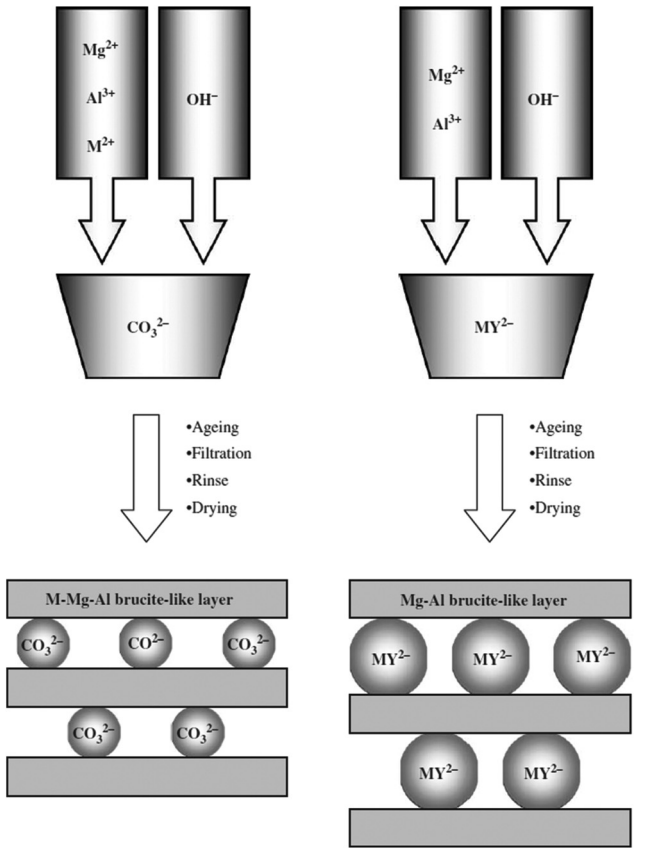

Fig. 5 Two ways for introducing M^{2+} metals into Mg–Al layered double hydroxides (MY^{2-} denotes the EDTA chelate of transition metal M^{2+}). Reproduced from ref. 75 with permission from Elsevier.

(M^{II} = Ni or Cu) with a small amount of noble metals, such as Pt, Rh and Ru.[77] For instance, Pt supported on an Mg(Ni,Al)O catalyst was reported as a self-activated/self-regenerated system during the CH_4 steam reforming reaction.[78] In this process, metallic Pt first favors the dissociation of the C–H bond to produce H atoms, which in turn migrate to the Mg(Ni,Al)O periclase surface by spillover and reduce Ni^{2+} to Ni^0 (self-activation). Later on, when Ni^0 gets oxidized to Ni^{2+} by steam, more hydrogen spillover supplied by Pt turns nickel back in its metallic state (self-regeneration).

3.3 Multifunctional catalysts

Nowadays, the necessity of intensified and environmentally friendly industrial processes has pushed the development of heterogeneous catalysts with multifunctional properties, where the desired product can be obtained in a one-pot reaction.[79] As was presented in sections 3.1 and 3.2, the LDHs and derived catalysts are characterized by multifunctional properties, going from the presence of acidic–basic sites with different nature and strengths, to the stabilization of metallic nanoparticles (both monometallic and bimetallic NPs). The design and fine-tuning of the specific functionalities will depend on the catalytic reaction for which the LDH-type catalysts will be used. In this manner, the combination of acidic–basic sites, as well as

metallic–basic active places, can be easily tailored by using an LDH-type structure.

As described in section 3.1, the acid–basic properties of HT-type materials can be fine-tuned by partially substituting Mg^{2+} by different cationic species and/or by playing with the Mg^{2+}/Al^{3+} molar ratio. This type of multifunctionality can be important, for instance, during the aldol condensation reaction of two different types of carbonyl compounds. Thus, whereas the role of the basic sites (Brønsted or Lewis) could be related to the deprotonation of the α-C atom of one of the carbonyl molecules to produce the respective carbanion, the acid sites (normally Lewis) could interact with the C=O group of the other molecule favoring its polarization and increasing the positive charge on the carbon atom of that carbonyl group. This situation drives the attack of the carbanion to form the respective adduct.[80] The multifunctionality plays also an important role when using noble and/or transition metal containing LDH derived mixed metal oxides (*e.g.* NiCuHT) in the Guerbet reaction, enabling the (de)hydrogenation, aldol condensation and dehydration steps involved.[81]

Next to this, the multifunctional properties related to the combination of metallic nanoparticles and the basic and/or acidic sites of the support are extremely important in order to face the different nature of the reagents and the reaction requirements involved in a one pot-reaction process.[81] In addition, metallic nanoparticles interacting with the active sites of the support can trigger the appearance of different type of metal-support interactions, which can be preponderant in both catalyst stability and catalytic efficiency.

4. Conversion of cellulose and hemicelullose derivatives into platform molecules

4.1 C5–C6 Sugars

4.1.1 Isomerization of glucose to fructose. Fructose is a renewable resource for the production of a versatile platform chemical, *i.e.*, 5-hydroxymethylfurfural (HMF), which can be converted into a number of value-added chemicals, and can be updated into liquid fuels. HMF can be synthesized by dehydration of any monosaccharide, but the reaction is more effective from fructose than from glucose or galactose.[82] Nevertheless, as glucose is a more available sugar, its isomerization into fructose appears to be an important step for the efficient formation of HMF as a platform molecule from renewables (Fig. 6).

The isomerization of glucose into fructose can be carried out with enzymes; however, this biological process has various drawbacks: (i) limiting operating temperature range, (ii) high-purity reactant, (iii) short life time of the enzyme compared to the inorganic catalyst, and (iv) high operating cost for mass production.[83,84] Therefore, significant efforts are devoted to designing selective inorganic chemical catalysts that can operate under a wider range of reaction conditions and at higher temperature in order to improve the reaction kinetics.

The base-catalyzed isomerization of glucose to fructose follows the Lobry de Bruyn–Alberda van Ekenstein (LdB–AvE) mechanism, named after the two scientists who discovered in 1895 that glucose is transformed into fructose in the presence of a base.[85] Although alkaline aqueous solutions of hydroxide salts have been used for glucose isomerization in the homogeneous phase,[86,87] the development of a solid catalyst for this process will facilitate a large-scale industrial operation enormously. For this reason and due to their basicity and stability properties, the utilization of hydrotalcites and derived materials has been highly considered recently for this reaction.

One of the first reports about the utilization of hydrotalcites for the isomerization of glucose into fructose was presented by Moreau *et al.*[88] in 2000. These authors compared the efficiency of alkaline-exchanged zeolites and calcined hydrotalcites (450 °C) for this reaction in water as a green solvent. Although most of the studied catalysts were based on different types of zeolites (A, X and Y) exchanged with Li^+, Na^+, K^+, Cs^+, Ca^{2+} or Ba^{2+}, the two analyzed hydrotalcites (Mg/Al = 2.5 and 3.0) showed the highest glucose conversion (up to 42% for Mg/Al = 3) and no detectable cation leaching during the reaction compared to severe cation leaching for the zeolites tested (12–30 wt% cation leaching) (Table 1). Unfortunately, the fructose selectivity of these hydrotalcite materials was not as good as the one observed in some of the exchanged zeolites (66% for Mg/Al = 2.5 hydrotalcite against 86% for the NaX zeolite) due to the strong basic properties of the LDH type material. Later on, Moreau *et al.*[89] showed that the nature of the interlayer anion in the LDH structure has an influence on the isomerization reaction and the basicity could be optimized for this reaction. Hydrotalcites in the OH^- form (synthesized by rehydration in decarbonated water) exhibit activity superior to materials in the carbonate form due to the higher basicity of the hydroxyl ion, which allowed a fructose selectivity of 83%, at 20% glucose conversion. In a similar way, Jung *et al.*[39,90] established that the reconstruction (rehydration) of a Mg–Al hydrotalcite provoked an augment in the number of weak basic sites compared to the as-synthesized material. In particu-

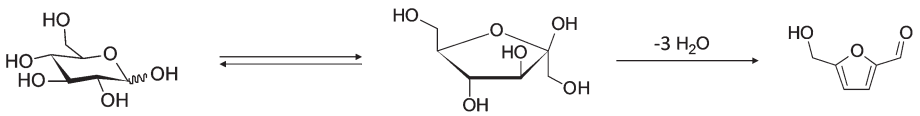

Fig. 6 Two-step D-glucose conversion into HMF.

Table 1 Overview on the catalytic efficiency of different solid basic catalysts for glucose isomerization into fructose

Entry	Catalyst	Solvent	T (°C)	Glucose conc. (wt%)	Glucose/cat. (wt)	X (%)	S (%)	Metal leaching (%)	Ref.
1	NaA Zeolite	H_2O	95	10	5	26	72	26	88
2	NaX Zeolite	H_2O	95	10	5	20	86	16	88
3	NaY Zeolite	H_2O	95	10	5	9	62	13	88
4	Fe_3O_4@SiO_2-TMG[a]	H_2O	120	20	4	46	54	n. a.	91
5	Mg/Al (2.5) calcined	H_2O	95	10	5	30	66	None	89
6	Mg/Al (3) calcined	H_2O	95	10	5	42	60	None	89
7	Mg/Al/(2.5) reconst[b]	H_2O	90	10	5	20	83	None	88
8	Mg/Al/(3.0) US reconst[b]	DMF	100	3	3	40	89	n.a.	39

[a] Magnetic base catalyst: tetramethylguanidine (TMG) immobilized onto silicon dioxide coated magnetic iron oxide. [b] With OH^- as intercalation anion (obtained *via* reconstruction in decarbonated water). US = reconstruction under ultrasound conditions; n.a. = not available.

lar, sonication assisted rehydration rather than mechanical stirring rehydration was more favorable for obtaining abundant weak basic sites, as it provoked a vertical breaking and exfoliation of the hydrotalcite layers.[39] The total basicity was examined by acrylic acid adsorption, while the strong basicity was measured by phenol adsorption. Correspondingly, the weak basicity was calculated by difference in the strong basicity and the total basicity. On the other hand, for the calcined material (Mg–Al–O mixed oxide), the presence of strong base sites (Lewis-type sites) was unfavorable for the isomerization of glucose into fructose. This result was related to the rapid decomposition of saccharides due to the strength of the basic sites on the catalyst.[39,89,90]

From the kinetic point of view, the isomerization of glucose into fructose is restricted due to the reversible character of the reaction ($K_{eq} \approx 1$ at 25 °C).[92] In order to shift the equilibrium of the reaction and to avoid the degradation of the desired product (fructose), Palkovits *et al.*[93] performed the isomerization of glucose into fructose under continuous operation conditions using a modified commercial hydrotalcite as a catalyst. This operation mode allowed a decrease in the generation of side products coming from the retro-aldol reaction of glucose and fructose (fructose was constantly removed from the reaction mixture), improving the selectivity of the reaction (up to 92% selectivity to fructose at 30% conversion) and favoring the stability of the catalyst. It is important to highlight that the best catalyst for this reaction was a hydrotalcite with a hydrophobic surface modification obtained by the introduction of sodium *n*-dodecyl sulfate between the brucite layers. Under long-term operation conditions (100 h time-on-stream), a slow deactivation of the catalyst was observed; nevertheless, the material can be easily regenerated by calcination at 500 °C and reconstructed in an aqueous phase solution of sodium *n*-dodecyl sulfate.

In 2015, Palkovits *et al.*[94] reported a very complete study on the utilization of Mg–Al hydrotalcites for the isomerization reaction of glucose, evaluating different parameters related to the structure-to-functionality properties of the material (Mg-to-Al ratio, crystallinity and structure, textural properties, morphology and basicity). The hydrotalcite with the highest concentration of basic sites was prepared by co-precipitation in aqueous medium at the isoelectric point of the hydrotalcite (pH 10), which produced a "sand-rose" type structure that favors the accessibility of the actives places for the reaction (Fig. 7). It was also shown that smaller crystallites and more dispersed primary particles of hydrotalcite could be obtained

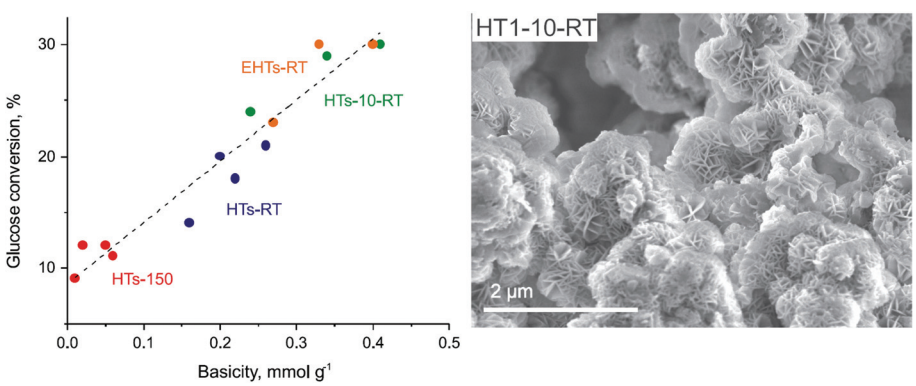

Fig. 7 Left: Glucose conversion *vs.* basicity of hydrotalcites. Reaction conditions: 5 mL of 10 wt% aqueous glucose solution, 100 mg catalyst, 110 °C, 1.5 h, 750 rpm. Right: SEM image of the "sand-rose" type morphology of HTs synthesized at pH 10. Reproduced from ref. 94 with permission from Elsevier.

by performing the synthesis of the materials in an aqueous-ethanol medium.

Recently a patent was published concerning ternary metal hydrotalcite materials with the composition of Mg : Al : Zn (3 : 1 : 1), Mg : Al : Cu (3 : 1 : 1) and Mg : Al : Sn (3 : 1 : 1) for the isomerization of glucose to fructose in water at 90 °C with yields between 22.3 and 29.4%.[95]

4.1.2 One-pot conversion of sugars to furans and furan derivatives. The combination of solid acid and basic catalysts for the one-pot synthesis of furan derivatives from saccharides (mono and disaccharides) has also been reported as a very efficient way to valorize cellulosic biomass.[96–100] In this approach, the coexistence of acid and base without neutralization allows the production of HMF from glucose *via* a tandem-type reaction. First, the glucose undergoes isomerization into fructose catalyzed by a solid base and then, fructose is dehydrated into HMF by a solid acid (as presented in Fig. 8). This one-pot reaction methodology was illustrated by using glucose as a monosaccharide, and Mg–Al hydrotalcite and Amberlyst-15 resin as base and acid heterogeneous catalysts, respectively, achieving 73% conversion of glucose and 58% selectivity to HMF under mild reaction conditions (100 °C, 3 h) and using DMF as a solvent.[96,101] Furthermore, due to the capacity of Amberlyst-15 to catalyze the acid hydrolysis of disaccharides, the utilization of sucrose (a disaccharide of glucose and fructose) and cellobiose (a disaccharide of glucose) to obtain HMF was also achieved by using the reported combination of acid and base catalysts. This catalytic system was also reported for the one-pot conversion of lactose (a disaccharide of D-glucose and D-galactose), D-arabinose and L-rhamnose for the synthesis of HMF, furfural and 5-methyl-2-furfuraldehyde (MF), respectively.[98]

In a more complex reaction system, a third heterogeneous catalyst (a hydrotalcite-supported ruthenium catalyst, Ru/HT) was implemented in order to drive the one-pot reaction to the selective oxidation of HMF into the corresponding dialdehyde, 2,5-diformylfuran (DFF) (a high-added value molecule), using glucose or fructose as saccharides[97] (Fig. 8). A high selectivity in the oxidation of HMF to DFF was observed by using an Ru/HT catalyst in the presence of molecular oxygen (up to 97% selectivity to DFF) in DMF solvent. Nevertheless, when the direct synthesis of DFF from fructose was performed in a one-pot system (using Amberlyst-15 and Ru/HT catalysts for dehydration and selective oxidation, respectively) a lower yield of DFF (13%) was produced due to the undesired side reaction of fructose decomposition by Ru/HT in the presence of oxygen. To overcome this problem, the authors implemented a two-step synthesis in a one-pot reaction where the Ru/HT catalyst was added into the initial reaction mixture (containing fructose or glucose; HT and/or Amberlyst-15 catalysts) after 3 h of reaction. Under these reaction conditions, the yield for the production of DFF was improved up to 49% using fructose and 25% using glucose.

More recently, the utilization of xylose for the one-pot synthesis of furfural and its derivatives has also been reported by using the combination of a heterogeneous Brønsted acid catalyst (Amberlyst-15) and a bi-functional (Lewis) acid–(Brønsted) base catalyst.[99,100] This reaction involves an aldose–ketose isomerization by the acid–base catalyst and successive dehydration of ketose by the Brønsted acid one. For this type of reaction, Shirotori *et al.*[99] reported that the utilization of the bi-functional catalyst Cr/Mg–Al, which consists of Brønsted base sites from the LDH structure and Lewis acid sites associated with the dispersed Cr_2O_3 species, was a better isomerization catalyst than bare Mg–Al LDH. These authors also reported the utilization of a different type of bi-functional acid–base catalyst by supporting M^{2+} species from aqueous solutions (M^{2+} = Mg^{2+}, Co^{2+}, Ni^{2+}, Cu^{2+} and Zn^{2+}) onto γ-Al_2O_3, which generates an M^{2+}–Al^{3+} LDH-type compound.[100] The highest yield to furfural, *i.e.* 46%, was achieved by using the combination of a Ni^{2+}-modified Al_2O_3 catalyst and Amberlyst-15.

5. Upgrading of cellulosic-derived platform molecules

5.1 Furfural

5.1.1 Hydrogenation. Furfural is a C5 compound with three double bonds and two oxygen atoms. Because of the high unsaturation, reduction with hydrogen is the most common approach to convert furfural to useful chemicals. Many compounds can be produced by the reduction of furfural: simple hydrogenation products (furfuryl alcohol and tetrahydrofurfuryl alcohol (THFA)), C–O hydrogenolysis products at the side chain (2-methylfuran and 2-methyltetrahydrofuran), decarbonylation products (furan and tetrahydrofuran), cyclo-

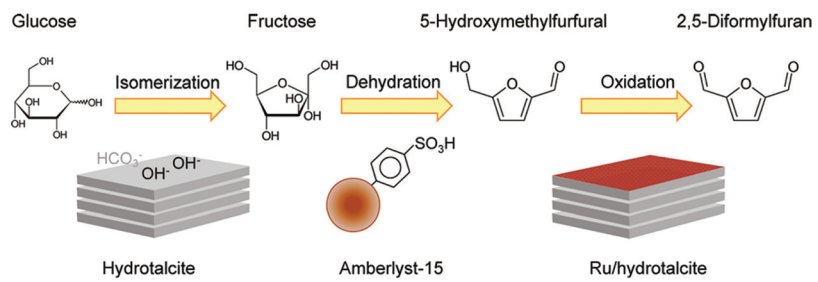

Fig. 8 One-pot synthesis of 2,5-diformylfuran from glucose through isomerization, dehydration, and selective oxidation. Reprinted with permission from ref. 97. Copyright 2011, American Chemical Society.

pentanone/cyclopentanol, and straight-chain C5 products[102] (Fig. 9). In this scenario, the utilization of layered double hydroxides as catalytic systems is mainly related to the capacity of these materials to produce highly dispersed metal-supported catalysts after the thermal activation/reduction of the LDH structure. One could classify these LDH-derived catalysts depending on the complexity of the supported metallic species (the active sites for the hydrogenation reaction) as monometallic or bimetallic systems.

In the case of monometallic systems, copper supported catalysts have been reported as active systems for the hydrogenation of furfural to furfuryl alcohol in gas and liquid-phase reactions.[103] The main advantage of using Cu for this type of reaction is the low cost and toxicity associated with this metal but also the selectivity of the hydrogenation process, which maintains the furanic structure and leads to furan derivatives, *e.g.* furfuryl alcohol.[104] Nevertheless, the dispersion of the metal species and their interaction with the support on these types of catalysts is very important in order to minimize the deactivation due to several factors related to the catalytic process, such as coke formation, change in the oxidation state, and sintering of metal particles, among others. Thus, the incorporation of copper into a layered double hydroxide structure to be used as catalyst precursor has been presented as an efficient way to prepare active and stable Cu-supported catalysts.

Villaverde *et al.*[105] studied the selective hydrogenation of furfural to furfuryl alcohol in liquid-phase over different Cr-free copper-based catalysts. Although all the evaluated catalysts (*i.e.* Cu/SiO_2, CuMgAl and CuZnAl) were able to achieve 100% selectivity to furfuryl alcohol at 383 K and 10 bar H_2, using propanol as solvent, the highest reaction rate was obtained on the CuMgAl catalyst derived from the respective copper-substituted hydrotalcite. The improved catalytic efficiency of this material was attributed to the metal-support interactions generated between the metallic copper particles and Mg^{2+} ions on the surface of a non-stoichiometric spinel-like matrix.

Copper catalysts derived from an LDH structure have also been used for a deeper hydrogenation of furfural in the aqueous-phase. Wang *et al.*[106] reported the utilization of the Cu/Zn/Al hydrotalcite-type precursor for the preparation of highly dispersed Cu supported catalysts for the hydrogenation of furfural to cyclopentanol. The calcination temperature used to decompose the layered precursor was found as a crucial parameter in order to achieve the best catalytic performance (100% conversion and 84% yield to cyclopentanol). It was observed that the material calcined at 600 °C showed the highest reducibility and metallic-copper dispersion after activation of the sample under hydrogen atmosphere (300 °C, 3 h). This behavior was attributed to the increased particle size of ZnO, facilitating at the same time the reduction of CuO species.

In a more recent report, Manikandan *et al.*[107] used the same type of hydrotalcite precursor to synthesize Ni-supported catalysts for the selective vapor phase hydrogenation of furfural at ambient pressure. One of the main issues related to the utilization of Ni supported catalysts for this reaction is the strong hydrogenation capacity of this metal, which favors the formation of tetrahydrofurfuryl alcohol instead of furfuryl alcohol.[108] Nonetheless, it was established that the surface synergistic interactions between the active metallic Ni sites and the strong basic sites from the hydrotalcite-derived support highly favored the selectivity of the reaction, achieving 95% selectivity towards the production of furfuryl alcohol, at 98% conversion (gas phase hydrogenation).[107] These authors remarked that the strong surface basic sites in close proximity

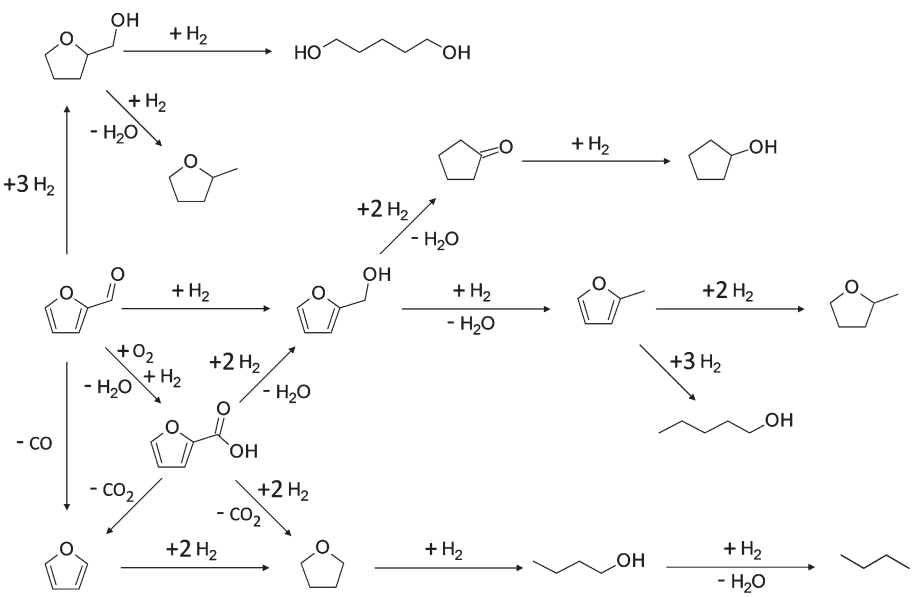

Fig. 9 Conversion of furfural to various value-added chemicals and biofuels.

with Ni^0 sites can interact with the π* acceptor orbital of the C═O group to enhance the reactivity of the carbonyl group. The uniform distribution of the Ni and Mg(Al)O species in the catalyst precursor was optimized by fine-tuning the Mg-to-Ni ratio used for the preparation of the LDH structure, which allowed an improved synergistic interaction between the involved active places.

In a recent patent of Thirumalaiswamy *et al.*[109] Ni-hydrotalcites prepared by co-precipitation followed by hydrothermal treatment are disclosed for the selective hydrogenation of furfural to furfuryl alcohol with conversion >89% and selectivity towards furfuryl alcohol >92%.

A catalyst consisting of hydrotalcite supported Pt nanoparticles (Pt/HT) has been reported as an efficient system for the direct hydrogenolysis of furfural to 1,2-pentanediol (1,2-PeD) without the presence of additives.[110] The selectivity of the reaction was highly favored by the cooperative effect of the Pt NPs and the basic sites of the HT structure. Initially, the Pt/HT catalyst reduces the formyl group of furfural to produce furfuryl alcohol. Then, C–O bond scissions of the furan ring of the alcohol, followed by hydrogenation, produce 1-hydroxy-2-pentanone and furthermore, 1,2-PeD. The surface basic sites of HT strongly interact with the hydroxymethyl moiety of the furfuryl alcohol intermediate generating alcoholate species, and the furan ring adsorbs onto the surface of the Pt NPs (Fig. 10).

Monometallic catalysts have been presented as highly active systems for the hydrogenation of furfural to fuel additives and value-added chemicals. Nevertheless, depending on the desired hydrogenation product and the type of metal, the selectivity of those types of catalysts can still be fairly low. Therefore, the addition of a secondary metal has been reported as a way to improve the properties of the first metal *via* the generation of synergistic and/or cooperative interactions. Considering the versatility of the LDH structure to incorporate different cationic and/or anionic species, the preparation of bimetallic catalysts derived from layered materials has also been reported for the selective hydrogenation of furfural. Ni–Cu hydrotalcite derived catalysts have been used for the selective hydrogenation of furfural to furfuryl alcohol in liquid phase.[111,112] The bimetallic catalyst was clearly more active than the corresponding monometallic ones (Cu–MgAlO or Ni–MgAlO), being able to achieve 93.2% conversion of furfural and 89.2% selectivity to furfuryl alcohol when loadings of 12.5 wt% of Cu and 4.5 wt% of Ni were used. In addition, the activation temperature was found to be very important in order to improve the catalytic activity and selectivity of the process. The presence of highly dispersed Cu^0 species was necessary to improve the catalytic activity, which was achieved by activation of the catalyst under hydrogen flow at 300 °C. Moreover the average Cu particle sizes in the reduced catalysts (3–4.5 nm) are much smaller and the percentage Cu dispersion values are larger than those of the supported catalysts, which shows that the catalysts with highly dispersed catalytic active centers can be obtained from hydrotalcite-like materials as precursors as compared to supported catalysts.

A similar Cu–Ni–Al hydrotalcite-based catalyst was used for the hydrogenation of furfural to cyclopentanone.[113] Up to 95.8% selectivity to cyclopentanone was achieved by fine-tuning the Cu : Ni : Al molar ratio of the catalyst (1 : 14 : 5, respectively) and the reaction conditions used for the hydrogenation process (140 °C, H_2 initial pressure of 40 bar and 8 h reaction).

Besides the bimetallic Ni–Cu LDHs-derived catalysts described before, few other reports have focused on the combination of one of these two transition metals (nickel or copper) with other different types of species, such as indium[114] and platinum.[115] Ni–In intermetallic compounds (IMCs) were prepared *via* the reduction of different types of LDH precursors described as Ni_xIn_y-LDHs, $Ni_xMg_yIn_z$-LDHs, Ni_3AlIn-LDHs and Ni_2AlIn-LDHs, and utilized as catalysts for the chemoselective hydrogenation of unsaturated carbonyl compounds, including the reaction of furfural to furfuryl alcohol.[114] The idea behind the design of these types of catalysts was to improve the preferential hydrogenation of the C═O group in the α,β-unsaturated aldehydes by combining (on the atomic scale) a highly active but low selective hydrogenation catalyst (nickel) with an inactive but more electropositive species (indium) *via* the formation of a Ni–In intermetallic compound. XAFS characterization and DFT calculation revealed the electron transfer and active-site isolation of the Ni–In IMCs accounting for the largely enhanced hydrogenation selectivity. It was found that the decrease of the Ni/In ratio leads to depressed catalytic activity but enhanced selectivity; for instance, a yield of 99% for the hydrogenation of furfural to furfuryl alcohol was achieved over the Ni_2In/Al_2O_3 catalyst (particle size 5.1 nm) at 110 °C and hydrogen pressure of 3.0 MPa (Fig. 11).

In a more recent report, Ren and co-workers[115] presented an innovative way to synthesize Pt–Ni/LDH-type catalysts by using a modified dealloying preparation strategy. This methodology requires the chemical etching of a Ni-rich Pt–Ni nanoalloy (octahedral shaped particles) in basic medium forming a

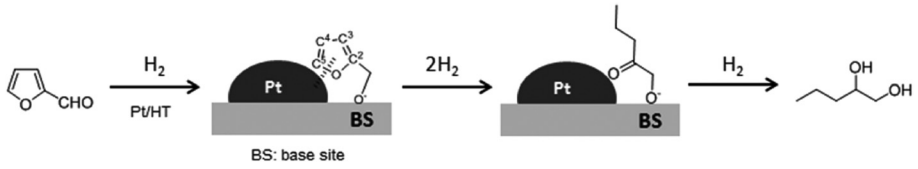

Fig. 10 Proposed reaction path for the hydrogenolysis of furfural to 1,2-pentanediol. Reprinted with permission from ref. 110. Copyright 2014, American Chemical Society.

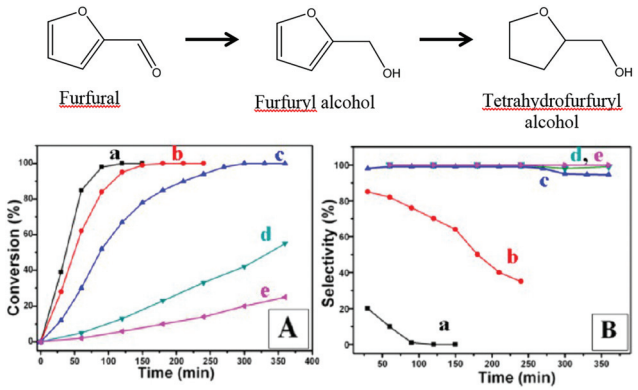

Fig. 11 (A) Catalytic conversion and (B) corresponding selectivity for the hydrogenation of furfural to furfuryl alcohol over different catalysts *vs*. reaction time: (a) Ni/Al_2O_3, (b) Ni_3In/Al_2O_3, (c) Ni_2In/Al_2O_3, (d) NiIn/3MgO, and (e) Ni_2In_3/7MgO. The reaction conditions are furfural/Ni ratio = 15; furfural, 1.0 mL; i-PrOH, 30 mL; temperature, 110 °C; and H_2 pressure, 3.0 MPa. Reprinted with permission from ref. 114. Copyright 2013, American Chemical Society.

nano-frame structure, followed by the *in situ* formation and decoration of NiAl-LDH on the frame surface. Then, during the hydrogenation of furfural, the combination of the surface basic sites on the LDH structure and the bimetallic Pt–Ni species prevent the generation of the hemiacetal intermediate, facilitating the hydrogenation of the C=O group in an active and selective way (TOF: 150 h^{-1} and 100% selectivity to furfuryl alcohol using a Pt_3Ni/LDH catalyst).

In general, it is difficult to establish a direct comparison between the catalytic activity of LDH-derived catalysts and "classic" metal-supported ones due the big diversity in reaction conditions reported in the literature. Nonetheless, as exemplified in Table 2, the implementation of LDH-derived catalysts allows the hydrogenation process to be performed under higher furfural concentrations and furfural-to-catalyst ratio than utilized with other metal supported catalysts. In the reactions with hydrotalcite catalysts, short chain alcohols (ethanol and isopropanol) were used as solvents, which can be seen as a greener alternative to the use of other organic solvents such as *n*-octane and toluene.

5.1.2 Aldol condensation. The aqueous-phase aldol condensation of furfural or hydroxymethyl furfural (HMF) with acetone has been reported as a primary step in the sustainable production of second generation biofuels from lignocellulosic biomass.[1,120] In this process, the C8 to C15 adducts obtained from the condensation process are transformed upon hydrogenation or a deep dehydrodeoxygenation step into jet fuel range alkanes (see Fig. 12).

In general, the aldol condensation is a C–C bond formation reaction in which an enol or enolate ion reacts with a carbonyl compound to form a β-hydroxyaldehyde or β-hydroxyketone, followed by a dehydration to give the corresponding α,β-unsaturated carbonyl moiety. Acids or bases can catalyze this reaction either in homogeneous or heterogeneous phase. Nevertheless, the tuning capability of the acidic–basic sites in LDH-type catalysts makes of these materials excellent candidates to selectively perform the reaction on an industrial scale.

In 2010, Liu *et al.*[121] reported the utilization of Mg–Al-LDH catalysts for the aldol condensation of furfural with acetone at 100 °C. These catalysts were prepared by rehydration of the corresponding mixed oxides, using different Mg/Al molar ratios (2, 2.5 or 3). The highest furfural conversion (78.6%) and selectivity to 4-(2-furyl)-3-buten-2-one (C8) of 72.3% was obtained using Mg–Al-LDH with an Mg/Al molar ratio of 2.5. It was also found that the calcination of these materials between 700 and 900 °C provokes the formation of a low crystalline spinel structure, which is active for the condensation of furfural and acetone. Nevertheless, the best selectivity observed on the rehydrated materials highlights the importance of the Brønsted-type basicity for this reaction. The same research group reported the preparation of a mesoporous Pd/cobalt aluminate bifunctional catalyst for the aldol condensation of furfural with acetone and the following hydrogenation of the condensation products.[122] The catalyst was prepared by the impregnation of Pd nitrate on a Co–Al–CO_3^{2-} hydrotalcite-like compound, followed by calcination at 300 °C (to obtain the cobalt aluminate) and then, reduction at 100 °C under hydrogen. The aldol condensation reaction achieved 98.9% conversion of furfural at 140 °C (5 h), with selectivity towards 4-(2-furyl)-3-buten-2-one (C8) and difurfurylideneactone (C13) of 69.2% and 30.8%, respectively. Afterwards, using the same catalysts, hydrogenation was conducted at 120 °C and 4 MPa

Table 2 Overview of the catalytic efficiency of different heterogeneous catalysts for the liquid-phase hydrogenation of furfural (FUR) to furfuryl alcohol (FOL)

Entry	Catalyst	Solvent	*T* (°C)	H_2 (Bar)	FUR conc. (wt%)	FUR/cat. (wt)	*X* (%)	*S* (%)	Metal leaching (ppm)	Ref.
1	Cu–Cr oxide	*n*-Octane	200	60	41	12	95	82	n.a.	116
2	Cu/Al_2O_3	H_2O	90	20	0.96	0.5	81	100	n.a.	117
3	Cu/SiO_2	Isopropanol	110	10	1.2	5.7	66	21	n.a.	105
4	Ni–Al alloy	None	100	7	100	10	100	100	n.a.	118
5	0.7%Pt–0.3%Sn/SiO_2	Toluene	100	20	16	29	63	100	None	119
6	Cu/Mg/Al calcined	Isopropanol	110	10	1.2	5.7	63	100	n.a.	105
7	Ni/Mg/Al calcined	Ethanol	200	10	33	34.5	56	53	n.a.	112
8	Cu–Ni/Mg/Al calcined	Ethanol	200	10	33	34.5	93	89	n.a.	112

n.a. = not available.

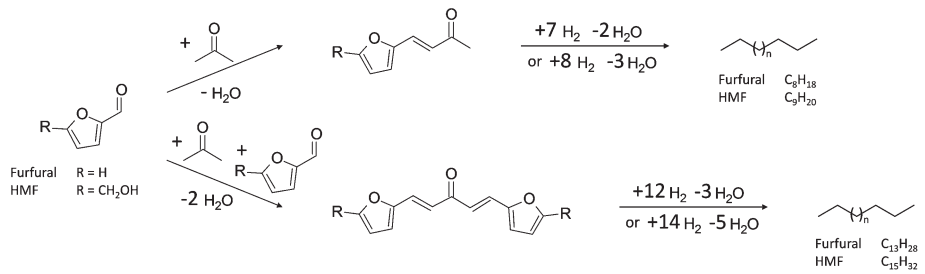

Fig. 12 Aldol condensation reaction of furfural and HMF with acetone.

of H_2, reaching a total furfural conversion of 99.0% and selectivity to 92.0% to the completely hydrogenated products (including the cyclized product).

Ordóñez *et al.*[123] studied the performance of a HT-derived mixed oxide (Mg_3AlO_x) for the aldolization of aqueous mixtures of furfural and acetone. Conversion of furfural and selectivity to C8 and C13 products was affected by the reaction conditions used. For instance, whereas the selectivity towards both C8 and C13 increased with time, the selectivity of the C8 fraction decreased as temperature augmented as a result of a serial reaction pathway. In addition, the distribution of the medium strength basic site (M^{n+}–O^{2-} pairs) studied catalyst showed to favor the production of dimeric condensation products rather than trimers (secondary condensation products).

More recently, Hora *et al.*[124] presented an extensive study of the influence of different preparation parameters of HT-based catalysts on their activity and selectivity in the aldol condensation of furfural with acetone. Three different activation procedures of the LDH structure were applied in order to obtain the desired catalyst: (i) calcination at 450 °C; (ii) *ex situ* rehydration of the calcined material (carried out in liquid or gas phase), and (ii) *in situ* rehydration of the calcined material (carried out in liquid phase). Different Mg/Al molar ratios were also considered (2, 3 and 4). The catalytic activity was affected by both, reaction temperature and Mg/Al molar ratio. In such a way, the best catalytic performance (>95% furfural conversion, 70% selectivity to the C8 dimer and 22% selectivity to the C13 trimer) was achieved at 100 °C and using an Mg/Al molar ratio of 3. It was also found that the *in situ* or *ex situ* rehydration of the catalysts affected differently the efficiency of the reaction depending on the Mg/Al molar ratio used. For instance, *ex situ* rehydration lowered the catalytic activity except on the catalyst with Mg/Al molar ratio equal to 2, and *in situ* rehydration caused catalyst activity improvement only in the case of the sample with Mg/Al molar ratio 3. This research group was also able to show that the aldolization reaction can be performed by using an industrial prepared Mg–Al HT-derived catalyst.[125] Despite the morphology and textural properties of the catalysts being different depending on the preparation method (a lower surface area was observed in the industrially prepared catalysts, which also affected the efficiency of the catalytic reaction), the basic properties of the samples were not influenced by this parameter. Still, the best catalytic performance was observed for the catalysts prepared with an Mg/Al molar ratio equal to 3.

Acidic zeolites, especially wide pore zeolites with a three-dimensional framework, show also some activity in the liquid-phase aldol condensation of furfural (FUR) with acetone with fairly high selectivity towards the C8 component. However during the reaction the zeolites suffer from carbonaceous deposits inside the micropores. Their catalytic properties can be restored completely after calcination above 500 °C.[126] As a comparison also the performance of MgO–ZrO_2 is given in Table 3. The selectivity to the C8 component 4-(2-furyl)-3-buten-2-one (46%) is lower than the selectivity to the C13 component difurfurylideneactone (57%). After catalyst recycling it retained most of its activity.[127]

5.2 Hydroxymethyl furfural (HMF)

5.2.1 Selective oxidation. 2,5-Furandicarboxylic acid (FDCA), a product obtained from the selective oxidation of HMF (see Fig. 13), is listed as one of the top-12 added-value

Table 3 Overview of the catalytic efficiency of different heterogeneous catalysts for the liquid-phase aldol condensation of furfural (FUR) with acetone

Entry	Catalyst	T (°C)	Pressure (bar)	Acetone/furfural (molar)	Furfural/Cat. (wt)	X (%)	S^a (%)	Cation leaching (ppm)	Ref.
1	HBEA	100	1	10	3.3	39	80	n.a.	126
2	MgO–ZrO_2	120	52 (He)	1	6	54	46	n.a.	127
3	Mg/Al (2.5) recont.	100	Autog.	10	4.8	79	72	n.a.	121
4	Pd/Co/Al calcined	140	1	10	6	99	69	n.a.	122
5	Mg/Al (3.0) calcined	50	10 (N_2)	1	n.a.	70	27	n.a.	123
6	Mg/Al (3.0) calcined	100	1	10	3.2	95	70	none	124

[a] Selectivity towards the dimer 4-(2-furyl)-3-buten-2-one (C8). n.a. = not available.

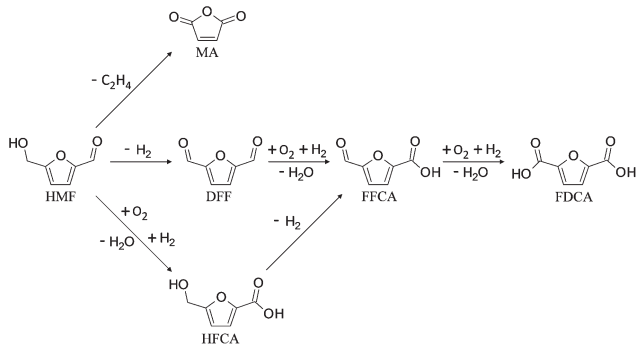

Fig. 13 Potential oxidation products obtained *via* the selective oxidation of HMF. Maleic anhydride (MA), 2,5 diformylfuran (DFF), 5-hydroxymethyl-2-furancarboxylic acid (HFCA), and 2,5-furandicarboxylic acid (FDCA).

chemicals from biomass by the US Department of Energy.[128] This molecule is considered a potential replacement of the petrochemical derived terephthalic acid for the synthesis of biobased polyesters. Therefore, the esterification product of ethane-1,2-diol and FDCA is polyethylene furanoate (PEF), a polymer with similar properties as the petroleum-based polyethylene terephthalate (PET).[129,130]

In 2015, Zhang and Deng[128] reviewed the most recent advances on the catalytic synthesis of FDCA and its derivatives. Although some new methods such as electrochemical oxidation and biocatalytic oxidation were reported for the synthesis of FDCA, the synthesis of this molecule was mainly carried out *via* chemical catalytic methods using homogeneous or heterogeneous catalysts. The catalytic aerobic oxidation of HMF to FDCA using heterogeneous catalysts in a basic reaction medium (*e.g.* NaOH or Na_2CO_3 solutions)[128] is considered one of the most sustainable alternatives, as oxygen is a cheap and environmentally friendly oxidant. In general, the activation of oxygen requires the use of highly active Pt, Pd, Au and Ru supported catalysts, whereas the presence of hydroxide ions is needed to facilitate the initial deprotonation of the alcohol function.[131,132] Nevertheless, the replacement of inorganic bases (such as NaOH) by highly basic catalytic supports is very desirable in order to avoid the formation of salts of carboxylic acid products during the oxidation of the alcohol and to point toward a greener catalytic process.

Ebitani *et al.*[133] developed a base-free process for the oxidation of HMF into FDCA using a hydrotalcite supported Au catalyst (1.92 wt% Au/HT). FDCA was achieved with a yield of 99% after 7 h at 95 °C under 1 bar O_2 in water. It was established that both the basicity of the support and the dispersion of the metal active sites played important roles in the oxidation of HMF. The influence of the basic HT support on oxidation was attributed to the formation of intermediate hemiacetals from aldehydes (HMF and FFCA) and formation of metal alcoholate species *via* a metal-hydride shift from HFCA. These authors also reported the reuse of the Au/HT catalyst without observing any leaching of gold. However, using a different catalyst configuration (a physical mixture of Au/TiO_2 and HT catalysts), Davis *et al.*[134] observed extensive leaching of Mg^{2+} from HT during the reaction. This situation was attributed to the chemical interaction between the basic HT and the formed FDCA.

In a patent of Yi and Zhang, hydrotalcite supported gold nanoparticles (Au/HT) and hydrotalcite supported palladium nanoparticles (Pd/HT) were used for the conversion of HMF to FDCA. Moreover, palladium modified hydrotalcite supported gold nanoparticles (Au_8Pd_2/HT) were highly active and showed excellent recyclability for 5 runs with FDCA yields of 98% to 99% using HMF.[135]

More recently, using the Operando Au L_{III}-edge XAS technique and detailed kinetic analysis, Ardemani and coworkers[136] described additional insights into the reaction mechanism of HMF to FDCA, using Au/HT-type catalysts and NaOH as a homogenous base. In the absence of soluble base, competitive adsorption between strongly bound HMF and reactively formed oxidation intermediates blocks gold sites. This situation can be overcome either by adding aqueous NaOH, which promotes solution-phase HMF activation, liberating gold sites able to activate the alcohol function within the metastable HFCA reactive intermediate, or by increasing the loading of gold in the Au/HT catalyst. 2 wt% gold loading was defined as the threshold between the use of homogeneous base and the totally heterogeneous catalyzed process (soluble base $\leq$2 wt% Au > solid base).

Lately, Ebitani *et al.*[137] reported the preparation of PVP (poly *N*-vinyl-2-pyrrolidone)-capped mono (Au, Pd, or Pt) and bimetallic (AuPd, AuPt, or PdPt) HT-supported catalysts for the base-free aerobic oxidation of HMF. Between the monometallic catalysts, Pt-PVP/HT (1 wt% metal loading) was found to be most active for FDCA formation (87% HMF conv., 35% FDCA yield), whereas the Au/HT catalyst was mainly selective to HFCA after 3 h reaction (69% HMF conv., 40% HFCA yield). Next to this, the bimetallic $Pt_{80}Pd_{20}$/HT catalyst showed the best catalytic performance among the whole series of studied catalysts, it being able to achieve 100% conversion of HMF after 4 h reaction (80% FDCA yield), and almost 100% yield of FDCA after 8 h reaction. XPS analysis evidenced an electronic transfer from Pd to Pt in the bimetallic nanoparticles supported on HT. Nevertheless, the exact nature of the structure/catalytic activity relationship is still under examination.

5.3 Levulinic acid

5.3.1 Hydrogenation (to obtain γ-valerolactone). Levulinic acid (LA) is a well-known product of hexose acid hydrolysis and it is inexpensively obtained by the decomposition of cellulose feedstock of glucose. Consequently, it is an attractive starting material for the production of many useful added-value chemicals. In particular, γ-valerolactone (GVL) has been proposed as one of the key components in biorefinery systems, because it can be used as an intermediate of many other chemicals (1,4-pentanediol, 2-methyltetrahydrofuran, and adipic acid), fuels and solvents.[138–140] GVL can be produced by the hydrogenation of LA (see Fig. 14) by using heterogeneous or homogeneous catalytic systems.[141] However, the development of

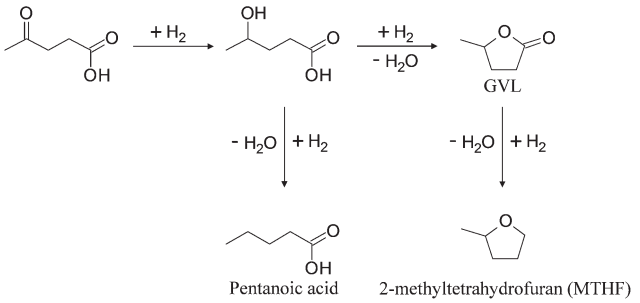

Fig. 14 Hydrogenation of levulinic acid.

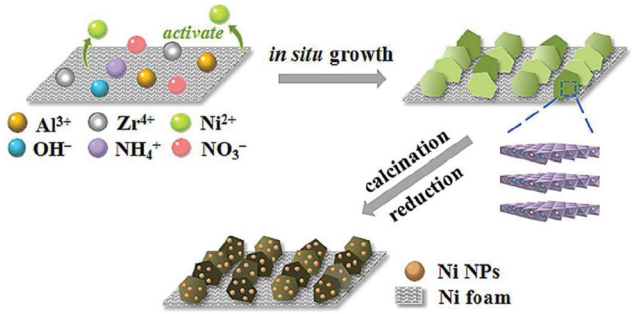

Fig. 15 Schematic representation of the fabrication of 3D structured nanowall-like Ni-based catalyst by a NiZrAl-LDH precursor route. Reproduced from ref. 144.

noble metal-free heterogeneous catalysts for this reaction (*e.g.* Cu and Ni-based catalysts) have become an important research target where the implementation of LDH-derived catalysts is attracting enormous attention in both batch and continuous reaction processes.

Yan *et al.*[142,143] reported the utilization of Cu-catalysts derived from hydrotalcite precursors as highly selective catalysts for the hydrogenation of levulinic acid to obtain GVL in aqueous phase. Among the different Cu-catalysts studied (Cu–Al, Cu–Cr, Cu–Fe) Cu–Cr hydrotalcite showed the highest selectivity, achieving 100% conversion and 91% yield towards GVL after 10 h reaction (T = 200 °C, 70 bar of H_2 pressure), whereas the worst catalyst was Cu–Fe hydrotalcite. This material achieved also 100% conversion of levulinic acid but a lower yield to GVL (81.5%) under the same reaction conditions. The authors attributed the catalytic differences to the electronegativity of the M^{3+} cation in the structure of HT (Al^{3+} = 1.61; Cr^{3+} = 1.66 and Fe^{3+} = 1.83). In such a way, the highest electronegativity of Fe^{3+} could induce a strong ability to attract electrons and promote further hydrogenolysis to 2-methyltetrahydrofuran. The same research group established that the highest catalytic performance could be reached by using a catalyst with a Cu^{2+}/Cr^{3+} molar ratio equal to 2 and they also performed recycling and stability tests for the Cr-containing catalyst.[142]

Recently, Li *et al.*[144] described the vapor-phase hydrogenation of levulinic acid over a structured nanowall-like nickel-based catalyst. This catalyst system was fabricated *via* a Ni–Zr–Al-LDH precursor route, involving the *in situ* growth of the Zr-containing precursor on the Ni foam strut through surface activation without an external nickel source (see Fig. 15).

The utilization of this structured catalyst allowed an excellent catalytic performance with the maximum GVL yield of 97.7% and productivity of 5.747 kg_{GVL} kg_{Cat}^{-1} h^{-1} (under WHSV = of 6.8 h^{-1}) at 250 °C, 0.1 MPa H_2 pressure and H_2/levulinic acid molar ratio equal to 4.0. These authors suggested a reaction mechanism involving the interaction of the well-dispersed Ni nanoparticles (NPs) with Lewis/Brønsted acid sites, which are mainly associated with the presence of Zr in the catalyst composition. Ni^0 NPs are responsible for the dissociation of hydrogen, whereas the Lewis acid sites nearby can serve as electron acceptors to polarize the carbonyl bond of the reactant, thus facilitating the production of the γ-hydrovaleric acid intermediate and then the intramolecular nucleophilic addition toward C (δ+) to form GVL. Besides, Brønsted acid sites can facilitate the ring-opening of GVL to produce pentenoic acid and further hydrogenation to valeric acid. Additionally, the utilization of a structured catalyst system characterized by open-cell structures favored heat transfer during the catalytic process and provided high tolerance to the weight hourly space velocity (from 0.6 up to 6.0 h^{-1}).

A Mn-containing spinel-supported copper nanocatalyst prepared *via* a Cu–Mn–Al LDH precursor route was also described for the gas-phase hydrogenation of biomass-derived compounds containing carbonyl groups (dimethyl succinate, acetol, levulinic acid, levulinic acid esters, and furfural).[145] Despite the fact that the catalyst was optimized for the hydrogenation of dimethyl succinate to γ-butyrolactone, it shows an excellent catalytic performance towards the selective hydrogenation of levulinic acid achieving a total conversion and 100% selectivity to GVL at 210 °C, 0.1 MPa H_2 pressure and LHSV = 1.8 h^{-1}. An exhaustive characterization of the catalyst showed that after activation of the LDH structure by oxidation and then reduction treatments, the catalyst surface is characterized by the presence of metallic copper nanoparticles in close interaction with Mn^{2+}–O_v–Mn^{2+} type bridges, where O_v represents the formation of an oxygen vacancy. In the proposed reaction mechanism, the carbonyl compound interacts with the Mn^{2+} surface species through the oxygen of the C=O group, weakening the strength of the bond. Then, Mn^{2+} are oxidized to Mn^{3+} by the C=O group, thus forming a C–O σ bond. Correspondingly, the oxygen vacancy linked to Mn^{2+} can be occupied by the oxygen atom of the C–O σ bond. Finally, the well-dispersed Cu^0 species adjacent to the surface defects dissociate H_2 for the hydrogenation reaction (see Fig. 16). The synergistic interaction between the Cu^0 NPs and the surface defects was highly favored by using the LDH structure as a catalyst precursor.

Additionally, Srinivasan and Gundekari[146] patented in 2016 a process for the preparation of GVL by the catalytic hydrogenation of levulinic acid in aqueous phase using Ru-based catalysts. Among the screened Ru-supported catalyst, Ru/MgAl-LDH material prepared by the wet impregnation of MgAl-LDH

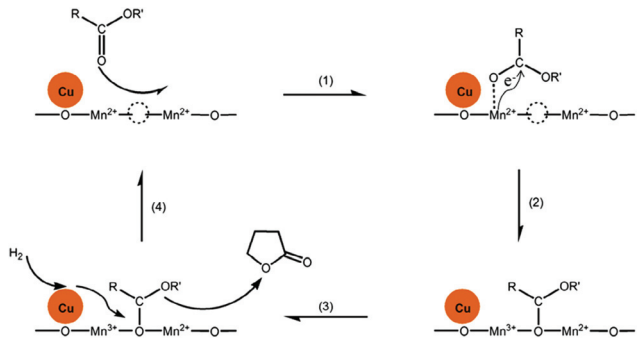

Fig. 16 A simplified reaction mechanism proposed in ref. 145 for the selective hydrogenation of biomass-derived carbonyl compounds over $CuMn_x$ catalysts. Reproduced with permission from Elsevier.

with $RuCl_3$ solution was able to achieve stoichiometric yields of GVL (~100%) under optimized reaction conditions (80 °C, 10 bar H_2 for 30 min). The main advantages of the invention claimed by the authors were: the excellent efficiency of the process in aqueous phase (100% conversion and selectivity), relatively short reaction times (2–30 min), no necessity of prior reduction of the catalyst (*in situ* generation of the active species), and catalyst recyclability. This LDH catalyst is very competitive compared to *e.g.* Cu/ZrO_2 and Cu/Al_2O_3 catalysts (see Table 4).[147]

Varkolu *et al.*[148] investigated on the vapor phase hydrogenation of levulinic acid (P = 1 atm; T = 250 °C) in the absence of external hydrogen, using supported Ni (30 wt%) catalysts over Al_2O_3, MgO and hydrotalcite (named as NA, NM and NHT for Ni/Al_2O_3, Ni/MgO and Ni/HT catalysts, respectively) and formic acid as a hydrogen source. Despite the three catalysts being active and selective for the production of GVL as the main reaction product, a significant decrease in the catalytic performance of NM and NHT catalysts was observed during the time on stream (up to 10 h). The authors suggested that the water generated during the reaction undergoes periclase-to-brucite transition in the Mg-containing supports (MgO and hydrotalcite), which provokes a drastic deactivation of these catalytic systems. Although this phase transformation does not occur in the NA catalyst (using Al_2O_3 as support), a slight decrease in catalytic activity as a function of time was also observed due to the carbon accumulation (coking) during the reaction.

5.4 Bio-ethanol

The term bioethanol refers to ethanol produced from biomass resources by biological processes (fermentation, enzymatic catalysis). In a more general sense, the term is also applied to all alcoholic liquors produced by the fermentation of sugars from plants, where the alcohol-to-water ratio on a molar basis is between 1 : 7 and 1 : 12. This bio-alcohol can be used directly as a fuel or as a blending component in gasoline.[150] However, the direct use of ethanol presents also several drawbacks including the need for engine adaptations, energy intensive separation techniques for water removal, *e.g. via* distillation, and a lower energy density.[151] As a result, recent research has focused on processes to upgrade ethanol,[152] for example, *via* steam reforming for the production of hydrogen and/or synthesis gas or by means of hydrogen-transfer processes yielding a broad spectrum of components.

5.4.1 Steam reforming. In industry, steam reforming is the most common hydrogen production process.[153] The fuel, in this case ethanol, is reacted with steam at high temperatures in order to produce hydrogen-rich gas which, for example, can be used in fuel cell applications. The overall ethanol steam reforming reaction is represented by eqn (1) and (2). This reaction is strongly endothermic and the reactor designs are typically limited by heat transfer, rather than by the reaction kinetics.[153,154] An alternative way of supplying heat to the reactor is to add oxygen or air to the feedstock. This oxygen will partially oxidize a fraction of the ethanol which is, for oxygen to ethanol molar ratios larger than 0.5, an exothermic reaction[155] (as represented in eqn (3) and (4)). This procedure is called oxidative steam reforming and can be performed at relatively low temperatures.

$$C_2H_5OH + H_2O \rightleftharpoons 4H_2 + 2CO \quad \Delta H^\circ_{298} = +256\ \text{kJ mol}^{-1}\ (ref.\ 61\ \text{and}\ 156) \tag{1}$$

$$C_2H_5OH + 3H_2O \rightleftharpoons 6H_2 + 2CO_2 \quad \Delta H^\circ_{298} = +174\ \text{kJ mol}^{-1}\ (ref.\ 61\ \text{and}\ 155) \tag{2}$$

$$C_2H_5OH + 0.5O_2 \rightleftharpoons 3H_2 + 2CO \quad \Delta H^\circ_{298} = +14\ \text{kJ mol}^{-1}\ (ref.\ 155) \tag{3}$$

Table 4 Overview of the catalytic efficiency of different heterogeneous catalysts for the liquid-phase hydrogenation of levulinic acid (L.A.) to γ-valerolactone (GVL)

Entry	Catalyst	Solvent	T (°C)	H_2 (Bar)	L.A. conc. (wt%)	L.A./cat. (wt)	X (%)	S (%)	Cation leaching (ppm)	Ref.
1	Cu/ZrO_2	H_2O	200	34	5	10	100	100	34	147
2	Cu/Al_2O_3	H_2O	200	34	5	10	100	100	174	147
5	Ru/Al_2O_3	Ethanol/H_2O	130	12	5	20	94	80	n.a.	149
6	Ru/SiO_2	Ethanol/H_2O	130	12	5	20	98	76	n.a.	149
7	Cu/Fe (2.0) calcined	H_2O	200	70	17	10	100	82	n.a.	143
8	Cu/Cr (2.0) calcined	H_2O	200	70	17	10	100	91	n.a.	143
9	Ru/Mg/Al uncalcined	H_2O	80	10	2.5	6.7	100	100	None	146

n.a. = not available.

$$C_2H_5OH + 1.5O_2 \rightleftharpoons 3H_2 + 2CO_2$$
$$\Delta H^{\circ}_{298} = -545\ \text{kJ mol}^{-1}\ (ref.\ 155) \quad (4)$$

Other major challenges of (oxidative) steam reforming are the formation of by-products and catalyst deactivation. Therefore, many research groups have been focusing on the development of highly active, selective and stable catalysts. Also in this field, metal supported catalysts derived from LDH materials are showing huge potential. Noble metal containing materials exhibit good catalytic performances and suffer less from deactivation than materials containing transition metals. However, the high cost of noble metals hinders their application. Therefore, increasing the stability of non-noble metal materials is an important goal in order to develop cheaper and more sustainable steam reforming catalysts.

Among transition metals, the high steam reforming activity and the relatively low cost of Ni makes it a suitable metal for the preparation of potential steam reforming catalysts.[157] In 2005, Velu *et al.*[158] reported a study of the catalytic activity of a series of Cu–Ni–Zn–Al-multicomponent mixed metal oxide catalysts with various Cu/Ni ratios, in the oxidative steam reforming of bio-ethanol. It was found that the ethanol dehydrogenation towards acetaldehyde is favored by the Cu-rich catalysts while Ni enhances the cracking of C–C bonds, producing CO, CO_2, CH_4 and H_2. At 300 °C, all investigated catalysts exhibit H_2 selectivities in the range of 50 to 55%. However, the stability or reusability of the materials were not investigated in this work.

Liu *et al.*[157] described the synthesis of Ni–Mg–Al mixed metal oxides *via* a combination of the reverse micro-emulsion and co-precipitation methods. Compared to materials synthesized *via* the traditional methods, these materials seem to exhibit superior characteristics in terms of catalytic activity, H_2 selectivity, catalyst stability, and the amount of carbon formation. The higher activity was attributed to high surface area, high thermal stability, and high dispersion of Ni particles. Strong interactions between metal and support increase the resistance against sintering and carbon formation, thus resulting in a higher stability.

Mixed oxide catalysts with a lamellar morphology have been obtained from crystallized Ni–Zn–Al and Ni–Mg–Al layered double hydroxides prepared using the urea hydrolysis method.[61] The mixed oxides obtained from Ni–Zn–Al LDHs are polyphasic, being a mixture of a rock salt phase (NiO), a wurtzite phase (ZnO) and a spinel phase (mostly likely $ZnAl_2O_4$), while the mixed oxides obtained from Ni–Mg–Al LDHs are monophasic, comprising a rock salt NiO–MgO solid solution. All catalysts exhibit a good steam reforming activity and no severe deactivation has been observed. However, both the amount of Ni as well as the substitution of Zn with Mg seem to have only a minor effect on the conversion and the product selectivities.

Coleman *et al.*[156] found that Mg–Al mixed oxide supported Ni exhibits a superior catalytic activity, H_2 and CO_x product selectivity and stability compared to the pure oxide supported nickel catalysts. Moreover, as can be seen in Fig. 17, the mixed oxide materials show no sign of deactivation after 20 h on stream. The improved catalytic performance was related to the incorporation of the pure oxides, MgO and Al_2O_3, into an $MgAl_2O_4$ phase. This prevents the incorporation of Ni in the support leaving it in its active form. In addition, $MgAl_2O_4$ exhibits moderate acidic and basic site strength and density compared to the pure oxide supported catalysts, reducing the reaction rate of the side reactions.

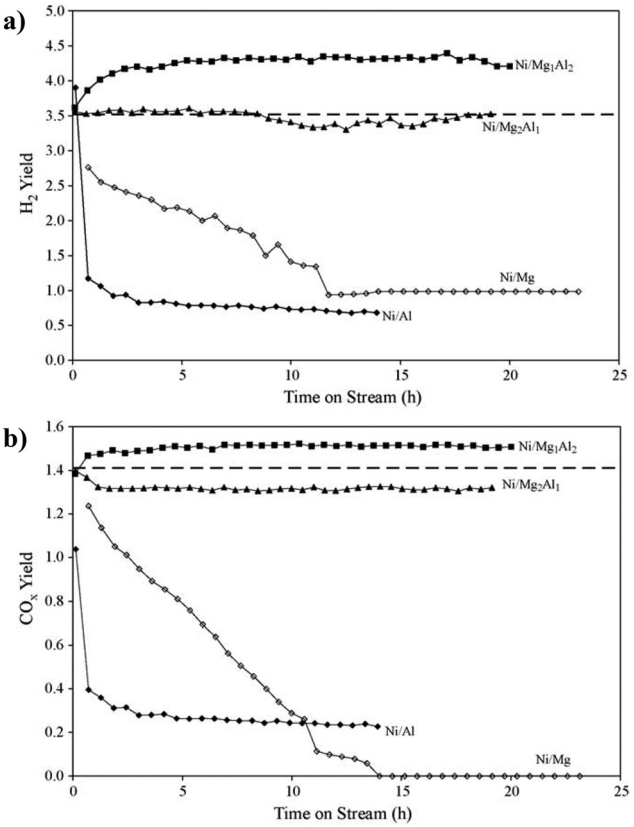

Fig. 17 (a) H_2 yield and (b) CO_x yield as a function of time-on-stream for pure and mixed oxide supported nickel catalysts evaluated at 500 °C, H_2O : EtOH = 8.4 : 1, GHSV = 260 000 $mL_{Feed}\ h^{-1}\ g_{cat}^{-1}$. The dashed line represents equilibrium expectation. Reproduced from ref. 156 with permission from Elsevier.

A study of a series of Co–Ni catalysts with varying composition demonstrated that the particle size and reducibility of the Co–Ni catalysts are affected by the degree of formation of a hydrotalcite-like structure, which increases with Co content.[159] The Ni catalyst displayed the strongest resistance against deactivation, while all the Co-containing catalysts exhibited much higher activities. The hydrogen selectivity was high and similar among the different catalysts.

Romero *et al.*[160] investigated the effect of the activation conditions on the surface and bulk composition and the catalytic performance of Ni–Mg–Al mixed oxides. The catalysts obtained by calcination at 600 °C and then reduction at 720 °C and those directly reduced at 720 °C showed the best catalytic performance. Similar research showed that a high reduction

temperature (>700 °C) promotes the reduction of Ni^0 metal, and effectively improves the catalytic activity and stability.[161] They found that the optimum reduction temperature is about 800 °C, at which a proper amount of Ni^0 species and good resistance to coke formation is obtained.

Bussi *et al.*[162] prepared NiLaZr and NiCuLaZr mixed metal oxide catalysts which are active in ethanol steam reforming. Both catalysts showed significant catalytic activity in the steam reforming of ethanol over the temperature range of 500–650 °C. Moreover, the NiCuLaZr catalysts exhibit a lower activity than their NiLaZr analogues, a fact the authors ascribed to the formation of a nickel–copper solution, with a lower catalytic activity in the cleavage of C–C bonds. However, it seems that at low temperatures, the catalysts are exposed to deactivation due to carbon formation.

Pirez *et al.*[155] studied H_2 production from ethanol on a cerium nickel based catalyst *via* steam reforming, partial oxidation and oxidative steam reforming. It is shown that a stable ethanol conversion and selectivity can be obtained at very low temperature when the material is first treated *in situ* in H_2 at 250 °C. The authors attributed this to the existence of an active site based on the formation of anionic vacancies and a mechanism involving a heterolytic abstraction of a hydride species from ethanol.

Co is, besides Ni, another transition metal with a lot of potential to be used for steam reforming catalysts. Typically, Co-based catalysts are cheap and active at low temperatures (523–823 K), but deactivate quickly due to coke formation. Espinal and coworkers[163] reported the preparation of robust honeycomb catalysts for bioethanol steam reforming based on calcined Co/Mg/Al hydrotalcites doped with potassium. The addition of potassium to the hydrotalcites reduces the number and strength of acid sites, which reduce at the same time coke formation derived from ethanol dehydration into ethylene. Bioethanol contains impurities derived from the fermentation process, which are more difficult to reform than ethanol. As a result, Co catalysts, typically, deactivate faster when bioethanol is fed.[164] However, these authors have shown that the stability of this catalytic system was exactly the same when using either ethanol or bioethanol in the feed-stream, achieving a stable gas phase composition up to 300 h time-on-stream (H_2 selectivity stabilized around 62%, CO_2 around 21%, CO and CH_4 around 5–8%).

Recently, Liu *et al.*[165] investigated a series of cobalt–cerium materials prepared by two methods. Because Co/CeO_2 (hp) prepared by homogeneous precipitation possessed a high BET surface area and small Co metal particles, Co/CeO_2 (hp) showed a higher ethanol conversion than the Co/CeO_2 catalysts prepared using the co-precipitation (cp) method and the impregnation (im) method. The selectivity of CO_2 over Co/CeO_2 (hp) increased with increasing reaction temperature from 300 to 400 °C, and decreased with increasing reaction temperature above 400 °C due to the increase of CO formation. The carbonaceous deposits formed on the catalyst surface during the reaction caused a slow deactivation in the steam reforming of ethanol over Co/CeO_2 (hp).

5.4.2 Hydrogen-transfer processes. The reduction of unsaturated organic compounds with an organic molecule instead of hydrogen gas or a metal hydride as hydrogen donor is known as hydrogen-transfer.[166] This review elaborates on alcohols and more specifically, (bio-)ethanol. The organic compounds which are most often converted *via* hydrogen transfer involving an alcohol are carbonyl compounds, nitriles and (other) alcohols (see Fig. 18).

Hydrogen-transfer reactions can be catalyzed by homogeneous metal complexes and heterogeneous acidic or basic materials are able to facilitate this process.[166–168] Literature has mainly focused on the former.[169–191] These homogeneous catalysts exhibit high turnover frequencies and selectivity. However, many of these metal complexes are very expensive and toxic. Moreover, these homogeneous catalysts require energy intensive separation processes. Hence, in the framework of sustainable catalysis, multifunctional solids such as hydrotalcites and derived materials can contribute to this research field. Below an overview of the most important research on the use of hydrotalcites in these types of reactions is given.

One of the first papers on the use of heterogeneous oxide catalysts for hydrogen-transfer involving carbonyl compounds and ethanol (see Fig. 18-1 to -3) was published in 1947.[192] The authors reported on the formation of butadiene from acetaldehyde and ethanol and the synthesis of styrene involving

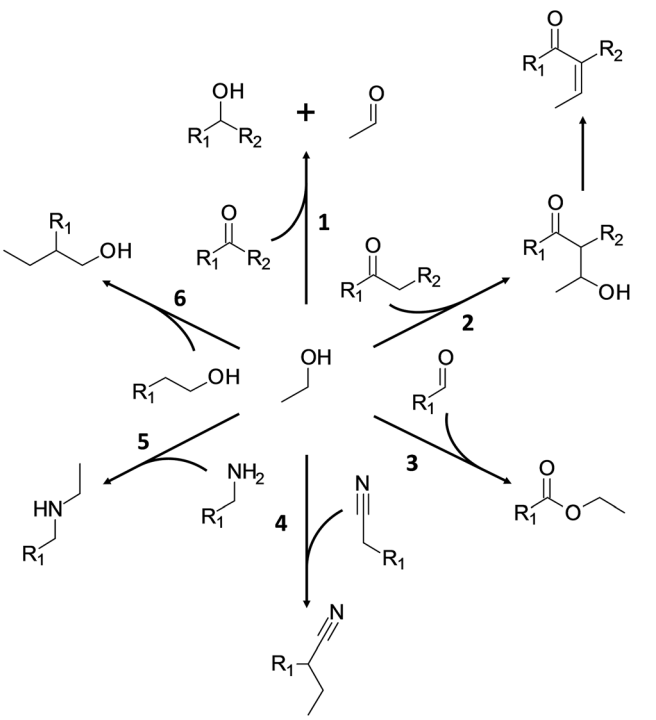

Fig. 18 General hydrogen-transfer reactions involving ethanol; (1) Meerwein–Ponndorf–Verley reduction of a carbonyl compound, (2) aldol condensation with a carbonyl compound, (3) Tishchenko reaction with an aldehyde, (4) alkylation of a nitrile, (5) alkylation of an amine and (6) Guerbet reaction with an alcohol.

the catalytic deoxygenation of acetophenone by ethanol. More than 5 decades later, Rao and coworkers[193] used a series of calcined layered double hydroxides as catalysts in the hydrogen-transfer of ketones with alcohols. They found that, compared to the other investigated materials, a layered double hydroxide with a 4 to 1 Mg : Al ratio catalyzes the reaction most efficiently. In another study, the same authors also applied various calcined hydrotalcites in the gas-phase reduction of propiophenone with isopropanol as the reductant. At high reaction temperatures (225–275 °C), reduction is followed by a dehydration, giving β-methylstyrene as the main product.[194] It is found that basic sites favor the initial hydrogenation to the alcohol, whereas the selectivity of β-methylstyrene is improved by the substitution of Mg^{2+} by Ni^{2+} or Cu^{2+} as a result of the formation of stronger acid sites. Consequently, with a calcined MgAl–CO_3^{2-} hydrotalcite, 1-phenyl-1-propanol is the main product (69% selectivity), whereas with a CuAl–CO_3^{2-}-derived mixed oxide, β-methylstyrene predominates. Aramendía *et al.*[195] used a series of basic catalysts consisting of magnesium oxide, calcium oxide, and mixed oxides obtained by the calcination of layered double hydroxides to perform the reaction between ethanol and benzaldehyde yielding phenol (see Fig. 18-1). However, also two other competing reactions were observed, *viz.* an aldol condensation yielding 3-pheny-2-propenal (see Fig. 18-2) and a Tishchenko cross-reaction yielding ethyl benzoate (see Fig. 18-3). The obtained selectivities of phenol, 3-pheny-2-propenal and ethyl benzoate were respectively, 70.3, 23.6 and 6.1%. Onyestyák *et al.* investigated the alkylation of acetone with ethanol using a neutral activated carbon, a hydrotalcite containing 9 wt% Cu and a hydrotalcite containing 5 wt% Pd.[196] Significant differences in yields of mono- or dialkylated ketones were observed. Additionally, it was observed that in a hydrogen atmosphere the ketone products could be reduced to alcohols. The authors concluded that Pd-hydrotalcite is the most promising for fuel production based on biomass fermentation.

In 2004, Motokura *et al.* reported the first α-alkylation of nitriles with alcohols, including ethanol, using heterogeneous catalysts, *i.e.*, ruthenium functionalized hydrotalcites (see Fig. 18-4).[197] The observed reaction rates were significantly higher than those of previously reported homogeneous Ru catalysts combined with a stoichiometric amount of Na_2CO_3.

In 2013, Dixit *et al.*[198] studied the catalytic activity of an Mg–Al hydrotalcite supported copper in the conversion of various alcohols in the aldol condensation with ketones (see Fig. 18-2) and the alkylation of amines (see Fig. 18-5). The catalysts showed excellent conversions in the range of 71 to 99% with high selectivity towards the alkylated products.

Various types of heterogeneous catalysts have been developed and patented for the Guerbet reaction.[199–201] The condensation of ethanol (self- and cross-condensation) by the Guerbet reaction have been reported under either batch or continuous operation mode, using different types of homogeneous, homogeneous/heterogeneous or totally heterogeneous catalytic systems.[202,203] In 1990, Ueda *et al.*[204] selectively synthesized propan-1-ol and 2-methylpropan-1-ol from methanol and ethanol at atmospheric pressure using different types of base-solid catalysts such as MgO, ZnO, CaO and M^{n+}-containing MgO catalysts (M^{n+} = Mn^{2+}, Cr^{3+}, Zn^{2+}, Al^{3+}, Na^{+} and Cs^{+}). Among them, MgO showed the best catalytic performance towards the Guerbet alcohols (up to 80% total alcohol selectivity), whereas ZnO was mainly selective to the dehydrogenation of ethanol to ethanal.

Ndou *et al.*[205] performed the dimerisation of ethanol over alkali earth metal oxides and modified MgO catalysts. They found that the MgO materials exhibit the highest catalytic activity and 1-butanol selectivity. Analysis of the possible reactions with the by-products showed that the reaction proceeds through a mechanism in which a C–H bond in the β-position in ethanol is activated by the basic metal oxide, and condenses with another molecule of ethanol by dehydration to form 1-butanol (see Fig. 19).[206] This is in strong contrast with the Guerbet reaction mechanism (see Fig. 19).

Tanchoux and coworkers[207] investigated the conversion of ethanol over Cu–Mg–Al mixed oxide catalysts obtained from layered double hydroxides. They found that the Mg/Al ratio does not significantly affect the catalytic properties of the studied catalysts. However, the copper content seems to play an important role. Optimal yields were obtained with materials comprising Cu loadings between 5 and 10 at.% with respect to the cationic species.

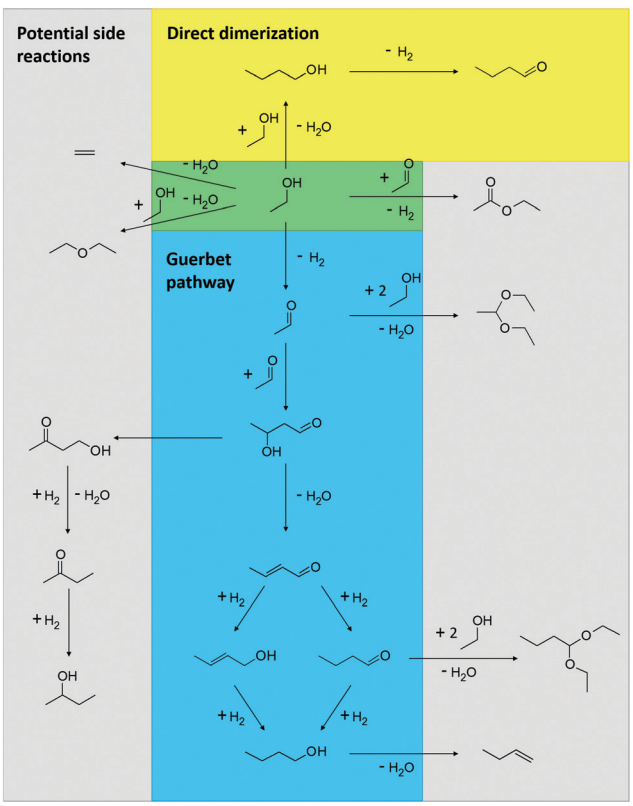

Fig. 19 Reaction scheme for ethanol transformation on hydrotalcite catalysts including potential side reactions.

León *et al.*[208] prepared three different hydrotalcite-derived mixed oxides, namely $Mg_6Al_2O_9$, Mg_6AlFeO_9 and $Mg_6Fe_2O_9$, by substitution of Al^{3+} by Fe^{3+}. This led to a slight decrease of the basic site concentration and a more pronounced decrease of the acid site concentration. Moreover, in case the catalyst in which the Al^{3+} cation is completely replaced by Fe^{3+}, the amount of acid sites is negligible. Accordingly, this material is the most selective catalyst for the formation of C_4 compounds, especially butanol. This has been ascribed to a strong decrease in the selectivity for ethanol dehydration, resulting in an increase of the formation of the dehydrogenation product, *i.e.*, acetaldehyde, which is the key reactant for the aldol condensation reactions. The same authors also investigated a series of Mg–Al mixed oxides prepared *via* different procedures.[209] These different procedures lead to different distributions of acid and basic sites and, hence, to different catalytic activities. Although the total conversion obtained with the different materials is rather similar, important differences are observed in the product selectivities.

A study of Mg and Al mixed oxides showed that adjacent acid and medium basic sites are needed in order to generate the intermediate compounds.[57] These acid–base pairs can be obtained by the insertion of Al in an MgO lattice or by incorporating Mg in a γ-Al_2O_3 lattice. The hydrogenation capacity increases with increasing Mg concentration. Strong basic sites and a specific superficial atomic arrangement seem not to be essential for the synthesis of C_4 from ethanol.

Riittonen *et al.*[210] screened 13 aluminium oxide supported metal catalysts for the valorization of bio-ethanol to 1-butanol. In terms of the selectivity towards 1-butanol, the investigated metals can be ranked as follows: Ni > Pt > Au ~ Rh > Ru ≫ Ag.

$CuMgAlO_x$ mixed metal oxides with Cu contents between 4 and 38 at.% prepared by the thermal decomposition of layered double hydroxides have been used for the vapor phase coupling of methanol and ethanol.[211] The incorporation of Cu in the mixed metal oxides drastically changed product selectivity, formation rates and catalyst stability. The conversion obtained using $MgAlO_x$ was rather low and the catalyst suffered from rapid catalyst deactivation. Moreover, higher alcohols were the predominant products. The conversion obtained using $CuMgAlO_x$ was significantly higher with minimal catalyst deactivation. The obtained product spectrum was much broader, including C–C coupling, *i.e.*, higher aldehydes, alcohols, and esters; non-C–C coupling, *e.g.*, acetaldehyde, methyl formate, methyl acetate, ethyl acetate; and decomposition products, *i.e.*, CO_x.

Shimizu and coworkers[212] investigated a series of supported nickel catalysts in the liquid phase self-coupling of aliphatic secondary alcohols. Effects of support material, *e.g.*, C, γ-Al_2O_3, SiO_2, TiO_2, ZrO_2 and CeO_2, and the oxidation state of Ni on activity are studied and it is found that both CeO_2 and metallic Ni are important for the reaction.

Tichit and coworkers[213] studied the effect of the inclusion of various metals, *i.e.*, Pd, Ag, Mn, Fe, Cu, Sm and Yb, in Mg–Al mixed metal oxides on the self-condensation of ethanol. It was shown that the nature of the cations modifies the ratio of acid and basic sites and, hence, strongly affects the catalytic performances. The highest butanol yields were obtained with the Pd-containing mixed oxide, which also exhibited remarkable catalyst stability.

Recently, Riittonen *et al.*[214] used Cu, Ni or Co deposited on a commercial mixed aluminum oxide as heterogeneous catalysts for the condensation of bio-ethanol to C_4 hydrocarbons. The different metals were found to yield significantly different product distributions. It was observed that a low copper loading and high nickel loading resulted in the formation of 1-butanol, whereas cobalt and high copper loading resulted in the production of ethyl acetate.

6. Conversion of lignin and lignin-derivatives into platform molecules

6.1 Lignin depolymerization

Lignin is a rather complex three-dimensional amorphous polymer based on hydroxyl-phenylpropane units issued from three monomers: *p*-coumaryl, coniferyl and synapyl alcohols differently distributed depending on the vegetal source (softwood, hardwood or grass)[215,216] (Fig. 20a). These structures are linked by a variety of interconnecting bonds, the β-O-4 linkages (β-aryl ether) being the predominant ones (Fig. 20b).

As lignin deconstruction can produce phenolic "platform molecules", the upgrading of this lignocellulose-fraction has attracted enormous attention during the past decade. Nevertheless, big difficulties in the catalytic processing of this biomass fraction due to the existence of a variety of different

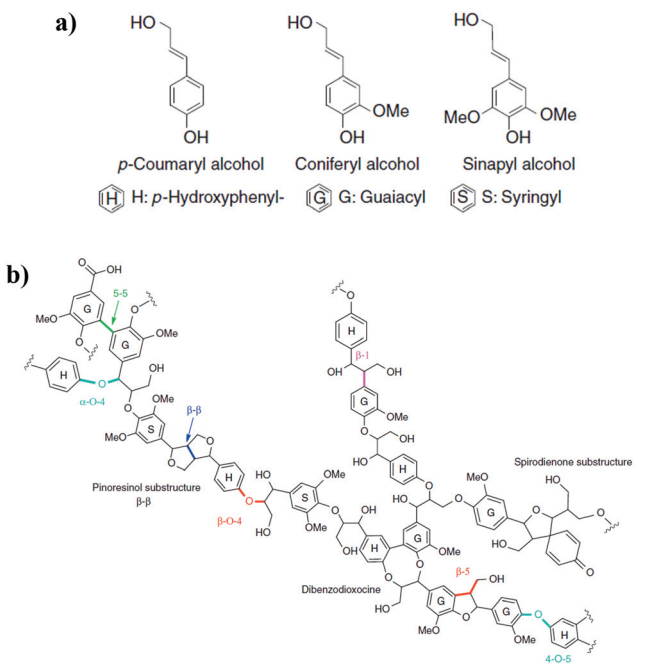

Fig. 20 (a) The three alcoholic monomeric units of lignin, and (b) example of a lignin structure with the typical 5–5, β–β, β-O-4, α-O-4, β-5, β-1 and 4-O-5 linkages. Reproduced from ref. 216.

interunit linkages, high affinity for the formation of a more condensed structure when thermochemically processed, poor product selectivity, and easy use as a solid fuel are the major barriers towards the development of lignin-based biorefining technologies.[217] In this context, LDHs and derived catalysts have been used for the depolymerization of lignin as a viable technology to produce aromatic platform molecules. Different types of model compounds (mainly (β-O-4 linkage ones) and reaction conditions have been reported).

In 2014, Beckham *et al.*[218,219] reported the cleavage of 2-phenoxy-1-phenyl ethanol (β-O-4 model) at 270 °C, using a Ni catalyst supported on an Mg–Al hydrotalcite (HT). In particular, a 5 wt% Ni/HT catalyst was effective for the cleavage of the C–O bond of the model dimer, without nickel reduction, demonstrating that NiO species dispersed on a solid basic support can effectively work as a lignin depolymerization catalyst. The high catalytic efficiency of this catalyst was attributed to the capacity of the nickel to provide a strong binding site for the aryl ether bond of the lignin model compound, whereas the hydroxide anions in the interlayer space of the LDH support were the active catalytic species.

More recently, the same research group reported on the utilization of different A^{n-}-exchanged hydrotalcites (A^{n-} = CO_3^{2-}; NO_3^-; OH^- or NO_3^{2-}/OH^- anions) for the β-O-4 bond scission of 2-phenoxy-1-phenylethanol, to produce phenol, acetophenone and 1-phenylethanol.[220] This study demonstrated that the LDH-catalyst characterized by the simultaneous presence of OH^- and NO_3^{2-} anions in the interlayer space can be as active as the Ni-supported material (Ni/HT). Although the role of the NO_3^- species in the catalytic process is still not totally understood, three main conclusions were presented for these types of catalysts: first, the nitrate is acting heterogeneously, as no significant catalytic activity was observed in the presence of homogeneous Ni^{2+}, NO_3^- and CO_3^{2-} species; second, the presence of nitrates favors the accessibility to the basic sites of the hydrotalcite, *i.e.* OH^- or even CO_3^{2-} anions, due to the generation of a larger interlayer spacing; and third, the nitrates present in the HT structure could also participate in the nitration of the benzylic OH group of the 2-phenoxy-1-phenylethanol as a key step in the mechanism of the reaction. The catalyst can be recycled until the NO_3^- anions are depleted, after which the activity can be restored by replenishing the NO_3^- reservoir and regenerating the HT structure.

Bolm *et al.*[221] also reported on the utilization of different transition-metal-containing HT materials for the oxidative cleavage of a lignin model compound, *erythro*-1-(3,5-dimethoxyphenyl)-2-(2-methoxyphenoxy)-1,3-propanediol, using molecular oxygen. Between the different transition metals studied (Co, Zn, Fe, Cu and V), the combination of Cu and V in the same HTC structure (a HT–Cu–V catalyst obtained by the intercalation of HT–Cu material with vanadate species) was very efficient in cleaving the β-O-4 linkage of the lignin model molecule, using either toluene or pyridine as solvents (conversion >99%). Nevertheless, only in the presence of pyridine was it possible to improve the product selectivity of the reaction to veratric acid and veratraldehyde as the main products. The authors also proved that, despite the reaction being heterogeneously catalyzed by the copper and vanadium species present in the HT-type catalyst (HT–Cu–V), this material also behaves as a dispenser of the catalytically active homogeneous species (as concluded from hot filtration experiments).

Barta *et al.*[222,223] described the development of a single-step approach for the hydrogenolysis–depolymerization of lignin and subsequent hydrogenation of aromatics, using a Cu-doped porous metal oxide derived from a LDH precursor as a catalyst and supercritical methanol as the reaction medium. This catalytic system favored the hydrogen transfer from methanol to the bio-oligomer organosolv lignin, provoking its breaking down to monomeric units *via* the hydrogenolysis of phenyl ether bonds, coupled with the hydrogenation of aromatic rings. In fact, the hydrogen equivalents needed for the reaction were produced *via* the methanol reforming and water-gas-shift activity of the multifunctional heterogeneous catalyst. No formation of char or other insoluble materials was claimed for this catalytic system. Barta *et al.*[223] studied this depolymerization reaction with Cu-doped porous metal oxide derived from a LDH precursor as catalyst in methanol with an added pressure of H_2. Catechols were obtained with high selectivity.

Hensen *et al.*[224–226] also reported the utilization of a solid-base catalyst, a Cu–Mg–Al mixed oxide derived from a LDH structure, for the one-step depolymerization/upgrading of lignin in the presence of supercritical ethanol. These authors found that the non-noble-metal oxide catalyst/ethanol system protects monomers and larger fragments (generated during the depolymerization process) from repolymerization (char formation) by alkylation with the solvent.[224,226] The role played by ethanol in this catalytic process is summarized in three main aspects (see also Fig. 21): (i) it serves as a source of hydrogen to facilitate lignin depolymerization and deoxygenation reactions by hydrolysis; (ii) ethanol acts as a scavenger for formaldehyde formed by removal of methoxy groups from lignin, thereby suppressing repolymerization reactions involving for-

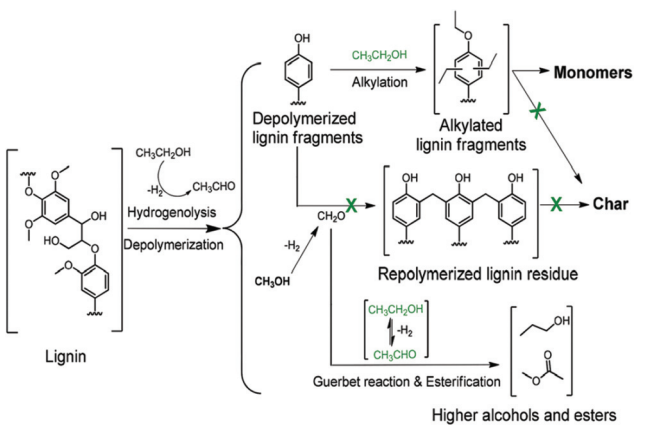

Fig. 21 The roles of alkylation, the Guerbet reaction, and esterification on suppressing char formation during lignin depolymerization over the $CuMgAlO_x$ catalyst in supercritical ethanol. Reproduced from ref. 226 with permission from The Royal Society of Chemistry.

maldehyde; and (iii) ethanol behaves as a capping agent to stabilize the reactive phenolic intermediates by O-alkylating the phenolic hydroxyl groups and C-alkylating the aromatic rings.

The same authors remarked that the main role of the Cu–Mg–Al mixed oxide catalyst in this process is to catalyze the reaction between formaldehyde and ethanol, limiting the polymerization reactions between phenolic products and formaldehyde.[225] The combination of copper and basic sites was presented as an efficient system to catalyze the associated Guerbet and esterification reactions, producing higher alcohols and esters from ethanol. In addition, the same combination of active sites facilitates the dehydrogenation of ethanol, producing hydrogen needed for hydrogenolysis and hydrodeoxygenation reactions. Furthermore, the Lewis acid sites associated with this type of catalyst (*i.e.* Cu^{2+} and Al^{3+} species) can catalyze C- and O- alkylation reactions, lowering the reactivity of phenolic fragments by the formation of heavy products.

6.2 Other lignin-related processes

Besides the chemical depolymerization of lignin, the potential of LDHs and derived catalysts for the valorization of this biopolymer starts to be explored in new, exciting subjects. For instance, because the thermal treatment of lignin can lead to the production of bio-syngas and/or bio-oil (*via* gasification or fast pyrolysis processes, respectively; see Fig. 2), the upgrading of these types of feedstock by using catalytic transformation routes is attracting enormous attention.[227,228]

6.2.1 Bio-syngas valorization. During the gasification of lignin, the biopolymer can be decomposed to syngas *via* partial oxidation at a high temperature. Subsequently, the obtained syngas, mainly consisting of small permanent gas molecules such as H_2, CO, CO_2, CH_4, H_2S and SO_2, can be converted into fuels and chemicals *via* processes such as Fischer–Tropsch synthesis. This process is well known and is typically used for the conversion of syngas obtained from the petrochemical industry. Several publications in the open literature have shown that hydrotalcites and related materials perform well in this reaction.[229–232] Typically, the catalytic materials contain either iron or cobalt as active component.

The composition of the bio-syngas obtained from lignin depends on the gasification temperature and pressure, the presence of steam and oxygen, heating rate, and the feed elemental composition.[233] Typically, the composition of syngas originating from a biomass feedstock deviates strongly from the composition of traditional syngas. The ideal syngas composition for the synthesis of fuels is a pure H_2/CO mixture with a H_2/CO ratio larger than 2.[234,235] Unfortunately, bio-syngas is H_2 deficient, with a H_2/CO ratio in the range of 0.3 to 2.0. Moreover, bio-syngas typically contains high amounts of CO_2 which is difficult to convert.[236,237] However, hydrotalcite-like materials are known to adsorb CO_2 and, hence, could potentially be used as combined catalytic and separation systems. Additionally, lignin often contains high amounts of sulphur originating from the separation process from biomass which, during gasification, leads to high concentrations of H_2S and SO_2. These sulphur components are known to be catalyst poisons, which impact downstream processes and, hence, should typically be removed to parts per billion (ppb) levels. However, Roberge *et al.*[238] investigated the sulfur-tolerance of cerium–cobalt mixed metal oxide catalysts in the water–gas shift reaction and found good catalyst stability. This clearly shows the potential of hydrotalcites and related materials in this field. However, more research is necessary to be able to cope with the significant different composition of bio-syngas compared to traditional syngas.

6.2.2 Catalytic steam reforming of tar. Besides the aforementioned gas molecules generated during biomass gasification, the raw product gas coming from the gasifier typically contains many contaminants. In particular, the presence of tar is highly undesirable. Tar is a complex mixture of condensable hydrocarbons, including single-ring to five-ring aromatic compounds along with oxygen-containing hydrocarbons and polycyclic aromatic hydrocarbons (PAH).[239] Many studies have shown that cellulose, hemicellulose and lignin produce different tar compounds.[23,240–243] Nevertheless, since only the lignin fraction of the biomass is aromatic in nature, lignin represents the main precursor for the formation of aromatic and PAH-type compounds.[243,244]

The formation of tar during the gasification process results in a significant decrease in efficiency and may cause serious problems, such as blocking and fouling in downstream equipment. In addition, tar is often responsible for serious coke deposition on the downstream catalysts provoking a rapid deactivation if the synthesis gas is utilized for production of methanol and Fischer–Tropsch liquids.[245]

Among the different methods proposed (including physical separation and thermal cracking), the catalytic steam reforming of tar (CSRT) has been described as the most promising route to remove tar from the gas product, since it can convert tar into syngas at temperatures equal to if not lower than the gasification temperature and without the production of waste water.[245,246] Thus, the implementation of this process has pushed the development of highly active and stable heterogeneous catalysts for this reaction. In particular Ni-based catalysts have been widely investigated for the steam reforming of tar, due to their low cost and high activity.[245,247,248] In many cases, Al_2O_3 is used as the support; however, the main problem with Al_2O_3 supported Ni catalysts is the deactivation caused by coke deposition and aggregation of metal particles. In order to decrease the coke deposition on the catalyst and increase the interaction of the metal species with support surfaces and modifiers (*e.g.* alkali species), several researchers have proposed the utilization of hydrotalcite-type precursors to prepare tar-reforming catalysts. An overview of the total carbon deposition on different tar-reforming catalyst is given in Table 5. For instance, Li and co-workers[249] reported the utilization of Ni/Mg/Al catalysts for the catalytic steam reforming of tar produced during the rapid pyrolysis of cedar wood. These catalytic systems were prepared from the calcination and reduction of hydrotalcite-like compounds. These authors

found an optimal catalyst composition (Ni/Mg/Al = 9/66/25 atomic percentage) for which a higher activity and coke resistance was observed (entry 1 in Table 5) compared to the reference Ni/MgO (entry 2 in Table 5) and Ni/Al_2O_3 (entry 3 in Table 5) supported catalysts. Additionally, the Ni/Mg/Al system showed an improved nickel reduction degree, whereas the order of Ni metal dispersion was estimated to be Ni/MgO > Ni/Mg/Al > Ni/Al_2O_3. Additionally, it was established that the particle size of the oxides used as supports in Ni/MgO and Ni/Al_2O_3 catalysts was much larger than that of Ni metal particles (after reduction). However, the reduction of Ni/Mg/Al mixed oxide provoked the formation of a nanocomposite-type structure that consisted of Ni metal particles and Mg(Ni,Al)O oxide particles with a similar size (~11 nm). The formation of the nanocomposite can enhance the large interface between Ni metal and oxide; at the same time, it can play an important role in the suppression of the aggregation of metal particles.

Tomishige *et al.* described the synthesis of Ni–Fe/Mg/Al bimetallic catalysts using the same preparation methodology (calcination and reduction of Ni/Mg/Fe/Al hydrotalcite-like compounds) for the catalytic steam reforming of toluene and phenol as model molecules,[250] and tar produced during the pyrolysis of cedar wood.[251] The authors reported the formation of uniform Ni–Fe alloy nanoparticles (average diameter = 9.5 nm) supported on Mg(Ni,Fe,Al)O mixed oxide characterized by a similar particle size (close to 13 nm). This means that they formed the same type of nanocomposite structure as described before. During the steam reforming of toluene, the Ni–Fe/Mg/Al catalyst (Fe/Ni = 0.25) showed an improved catalytic activity and stability after 20 h of reaction, keeping a 99% conversion of toluene with a total carbon deposition of 15 $mg_C\ g_{cat}^{-1}$ (entry 4 in Table 5). On the other hand, the monometallic Ni/Mg/Al catalyst showed around 77% conversion of toluene and carbon deposition caused a pressure drop after 17 h of reaction (total carbon deposited after 20 h = 750 $mg_C\ g_{cat}^{-1}$, entry 5 in Table 5). According to the authors, the formation of Ni–Fe alloy nanoparticles results in Ni–Fe bimetallic sites where nickel atoms can activate hydrocarbon molecules and neighboring iron atoms can activate H_2O to H_2 and adsorb oxygen atoms. The oxygen atoms supplied by iron react with adsorbed hydrocarbon, leading to high activity and resistance to coke formation.[250] This Ni–Fe bimetallic catalyst (entry 6 in Table 5) exhibited also a higher activity and resistance to coke deposition in the steam reforming of tar (from pyrolysis of cedar wood) than monometallic Ni/Mg/Al (entry 7 in Table 5) and Fe/Mg/Al (entry 8 in Table 5) catalysts.[251] Even more, the Ni–Fe alloy NPs on Ni–Fe/Mg/Al catalyst displayed a much better regenerability towards the oxidation–reduction treatment than those supported by the conventional α-Al_2O_3-supported catalyst. The oxidation treatment of the Ni–Fe alloy NPs induces the incorporation of Ni and Fe ions into the near surface of Mg(Ni, Fe, Al)O periclase and subsequent reduction of the Ni and Fe ions regenerates uniform Ni–Fe alloy NPs. More recently, the same research group studied the reactivity and stability of the optimized Ni–Fe/Mg/Al (Fe/Ni = 0.25) catalyst for the steam reforming of different tar model compounds: benzene, toluene and phenol.[252] In the case of benzene and toluene steam reforming, the Ni–Fe bimetallic catalyst (entries 9, 11 and 13 in Table 5) showed a much better activity and coke resistance as compared with the monometallic Ni/Mg/Al catalyst (entries 10, 12 and 14 in Table 5). Nevertheless, when phenol was used as a substrate, a large amount of carbon

Table 5 Overview of the total carbon deposition on different solid basic catalysts for tar steam reforming

Entry	Catalyst	Reactant	Temp. (°C)	Molar steam/C (–)	Time on stream (h)	Total carbon deposition (mg g_{cat}^{-1})	Ref.
1	Ni/Mg/Al (9/66/25)	Tar	650	0.5	1	38	249
2	Ni/MgO	Tar	650	0.5	1	65	249
3	$NiAl_2O_3$	Tar	650	0.5	1	166	249
4	Ni–Fe/Mg/Al (Ni/Fe = 0.25)	Toluene	600	1.7	20	15	250
5	Ni/Mg/Al	Toluene	600	1.7	20	750	250
6	Ni–Fe/Mg/Al (Ni/Fe = 0.25)	Tar	550	0.38	0.25	120	251
7	Ni/Mg/Al	Tar	550	0.38	0.25	171	251
8	Fe/Mg/Al	Tar	550	0.38	0.25	258	251
9	Ni–Fe/Mg/Al (Fe/Ni = 0.25)	Benzene	600	1.7	1.33	5	252
10	Ni/Mg/Al	Benzene	600	1.7	1.33	223	252
11	Ni–Fe/Mg/Al (Fe/Ni = 0.25)	Toluene	600	1.7	1.33	17	252
12	Ni/Mg/Al	Toluene	600	1.7	1.33	158	252
13	Ni–Fe/Mg/Al (Fe/Ni = 0.25)	Phenol	600	1.9	1.33	36	252
14	Ni/Mg/Al	Phenol	600	1.9	1.33	165	252
15	Co/Mg/Al (10/40/50)	Tar	600	0.23	1	36	253
16	Co/α-Al_2O_3	Tar	600	0.23	1	110	253
17	Co–Fe/Mg/Al (10–10/40/40)	Tar	600	0.23	1	37	254
18	Ni–Cu/Mg/Al (Cu/Ni = 0.25)	Tar	650	0.38	0.25	93	255
19	Ni/Mg/Al	Tar	650	0.38	0.25	171	255
20	Ni/Mg/Al	Tar	850	2.9	0.5	115.3 (inlet) 15.4 (outlet)	256
21	Ni–Cu/Mg/Al (Cu/Ni = 0.25)	Tar	850	2.9	0.5	44.8 (inlet) 9.1 (outlet)	256
22	Pd–Ni/Mg/Al (Pd/Ni = 0.0023)	Tar	650	0.5	2	14	257

derived from the decomposition of phenol was deposited on Ni–Fe/Mg/Al catalyst even with high (3.8) S/C ratio. The authors proved that phenol was strongly adsorbed onto the Fe site as well as the Ni site, and the adsorbed phenol could be converted into carbonaceous species under the reaction conditions.

The catalyst synthesis route based on the calcination and reduction of hydrotalcite-like precursors was implemented for the preparation of monometallic Co/Mg/Al catalysts (entry 15 in Table 5)[253] and bimetallic Co–Fe/Mg/Al (entry 17 in Table 5)[254] and Ni–Cu/Mg/Al catalysts (entries 18 and 21 in Table 5).[255,256] Although the Co/Mg/Al catalyst showed a better catalytic performance (activity and coke resistance) during the catalytic reforming of tar than that observed by Ni/Mg/Al (entries 19 and 20 in Table 5) and Co/α-Al_2O_3 (entry 16 in Table 5), in all the cases the bimetallic catalysts showed an improved catalytic performance compared with the monometallic catalysts (classically supported and hydrotalcite derived ones). This positive effect was generally correlated to a cooperative effect between the two metal species, which decreases the coke deposition during the reaction. Similarly, Chen *et al.* showed that adding a small amount of palladium improves the catalytic activity and coke resistance (entry 22 in Table 5).[257] On the other hand, the modification of a Ni/Mg/Al catalyst with a small amount of palladium (0.05 wt%) showed to be an effective way to improve the reducibility and dispersion of Ni during the reductive activation of the catalyst (improving the catalytic performance), but also Pd was found to avoid the re-oxidation of Ni during the course of the steam reforming reaction.

6.2.3 Hydrodeoxygenation process (HDO). Lignin-derived bio-oil can be formed *via* a fast-pyrolysis treatment of the lignin feedstock. During pyrolysis, lignin decomposes into the vapor phase at 280–500 °C, forming polysubstituted phenolic monomers and oligomers *via* ether and C–C bond cleavage. To achieve relatively high liquid product yields and to decrease char formation, high temperatures and short reactor residence times are favorable.[228] The condensed bio-oil typically contains significant amounts of lignin-derived phenolic molecules (*e.g.* guaiacyl, syringyl, and hydroxyphenyl derivatives), which, once converted into aromatics and alkanes, constitute a valuable source of hydrocarbon fuel components.

Several catalytic routes have been proposed to upgrade lignin-derived bio-oil (such as zeolite upgrading to produce hydrocarbons and aqueous phase reforming to produce H_2).[227] However, the hydrodeoxygenation process (HDO) is one of the most common methods to achieve oxygen removal. HDO involves the treatment of oxygen-containing molecules with high-pressure H_2 at moderate temperature (200–500 °C) in the presence of heterogeneous catalysts. During HDO, C–O bond cleavage *via* hydrogenolysis with H_2 removes oxygen in the form of water. The saturation of aromatics by hydrogenation, and other reactions (such as C–C bond cracking, isomerization, and dehydration) also occur.[258]

Most of the literature reports consider the utilization of hydrotreating catalysts like supported Co(Ni)MoS, for the HDO reaction of phenolic compounds such as guaiacol (2-methoxyphenol) and eugenol (2-methoxy-4-allylphenol).[228] The utilization of acidic supports (*e.g.* γ-Al_2O_3 or SiO_2–Al_2O_3) is normally considered for these types of catalysts because the acid sites are active for deoxygenation reactions. Nevertheless, in 2012, Delledonne and co-workers[259] patented the utilization of a new family of polymetallic sulfided catalysts supported on (at least) slightly basic materials for the conversion of lignin to hydrocarbons. For instance, a sulfided Ni(4%)Mo(10%) catalyst supported on an Mg–Al mixed oxide derived from a commercial HT (Plural MG70 Codea/Sasol) was used for the hydrocracking/hydrodeoxygenation process of Acetosolve lignin. After 4 h of reaction at 390 °C and 4 MPa H_2 pressure, 55% of deoxygenation was achieved.

Next to this, in the recent years the development of supported noble-metal catalysts (Ru, Pd, Pt, and Rh, and their alloys) has been reported as effective non-sulfide-based HDO catalysts for bio-oil upgrading.[227] Nevertheless, to the best of our knowledge, neither LDH nor derived mixed oxides have been used as catalytic supports for these metals in the HDO reaction of lignin-derived bio-oil. However, a recent literature report described the utilization of a metal–solid base bifunctional catalyst (Ru/ZrO_2-$La(OH)_3$) for the partial HDO reaction of guaiacol to obtain cyclohexanol.[260] These results open new perspectives for the utilization of LDH and derived mixed oxides in the HDO field, although also the stability of these types of materials in an aqueous phase has to be considered.

7. Conclusions, challenges and perspectives

Besides their important role in the refining and petrochemical industries, LDH and derived materials have also been playing a relevant function in the development of biomass valorization processes, where lignocellulose emerges as the most promising and sustainable bio-source to produce chemicals and fuels.

Due to the complexity and diverse nature of the lignocellulosic feedstock, many different transformation routes must be considered and strategically integrated into a biorefinery scheme. Here, we have tried to identify some of the most relevant catalytic processes involved in a lignocellulosic-biorefinery scheme having in mind the implementation and development of LDH and derived materials as rational-designed heterogeneous catalysts. In particular, the structure-to-functionality properties of these materials, their versatility in composition and preparation routes, and their capability to be integrated in multicomponent systems (such as three-dimensional structured catalysts and membrane reactors) could be extrapolated as the most remarkable features of this family of catalysts for the catalytic upgrading of bio-resources.

Next to this, the LDH structure is presented as an excellent platform to produce cheap and robust catalysts facilitating the dispersion and stabilization of different cations such as: Cu^{2+}, Ni^{2+}, Co^{2+}, Cr^{3+}, and Pd^{2+}, among others. This feature allows

an optimization of metal loading in the case of metal supported catalysts, the NP size in case of reduction treatment and also facilitates the generation of synergistic interactions between the catalyst components that can drive selectivity during the catalytic reaction. The LDH and derived structures are very versatile materials that can contain (de)hydrogenation centers as well as Brønsted and/or Lewis sites and the specific composition and interactions can be fine-tuned upon their preparation and thermal treatment, metal loading and metal(s) choice. Dispersion of metal species and interaction with the support are also important to provide stable catalysts (low deactivation from coke and low sintering of metal particles) enabling good durability.

In addition, some innovative catalytic processes using LDHs and derived catalysts start to be described for the upgrading of lignocellulose-derived molecules. For instance LDHs can be used to catalyze (oxidative) steam-reforming reactions in order to convert bio-ethanol in hydrogen-rich gas which, for example, can be used in fuel cell applications. This is a field that has been studied exuberantly during the past ten to fifteen years. However, a few papers focusing on more complex systems, such as hydrotalcite-type materials coated onto ceramic honeycombs, selective membrane systems or catalyst-sorbent multilayer pattern arrangements, have been published. Most recently, in 2016, a series of modified LDH-derived ferrospinels were used in an alternative route to produce hydrogen from ethanol, *i.e.*, chemical-looping reforming.[261] These alternative systems show promising results paving the way for future research.

Additionally, multifunctional catalysts can also play a significant role in hydrogen-transfer processes involving bio-ethanol yielding a broad spectrum of components. A substantial amount of research has been performed on the use of this type of materials in the Guerbet reaction between ethanol and other alcohols. However, the use of these types of materials in other interesting processes involving hydrogen-transfer reactions with ethanol, such as the α-alkylation of nitriles and the alkylation of amines, has been poorly investigated. Hence, many research opportunities can still be found in this area.

On the other hand, the valorization of lignin gasification and fast pyrolysis products (*i.e.* syngas and lignin-derived bio-oil, respectively) remains a challenging topic due to the complexity and high oxygenation degree of the feed and the presence of sulfur-containing molecules that act as catalyst poisons. Nevertheless, LDH-like materials could potentially be used in gasification and fast-pyrolysis processes as CO_2 adsorbents/catalysts, favoring yields and decreasing CO_2 emissions. Moreover, cerium–cobalt mixed metal oxide catalysts exhibit a remarkable sulfur-tolerance in the water–gas shift reaction proving the high potential of these materials to cope with bio-syngas containing high amounts of sulfur.[238]

LDH-like materials have also been recently reported as selective CO_2 adsorbents for the upgrading of biogas.[262] Nevertheless, because competitive and cheaper materials such as CaO are also used for this application, improvements in the cost-to-functionality relationship must be considered in the case of LDHs.

Another important aspect to be considered for the implementation of these types of catalysts in biorefinery-type processes is the simplicity and scalability of their preparation methods. The most conventional method is the co-precipitation of the metal salts from a mixed solution at room temperature and constant pH. Nevertheless, for a large-scale production of LDH-type catalysts this preparation route would provoke the production of large amounts of wastewater and noxious gases. To fit the utilization of these materials within green and scalable preparation methodologies, Fahami *et al.*[263] recently reported the use of a mechanochemistry process for the synthesis of Mg–Al-LDHs. This methodology can facilitate the mass production of LDH-type materials, keeping the production cost low, and even more important, diminishing the generation of waste products during the process.

One of the biggest concerns to be overcome by mixed metal oxides derived from LDH precursors is their stability in the presence of water. Due the reconstruction of the layered structure in the presence of water, the stability of the calcined catalysts can be affected in an aqueous reaction medium or by the water generated as a side-product. The periclase to brucite transition in contact with water can cause deactivation. Nevertheless, by using different reaction configurations (the presence of Dean–Stark systems and/or water scavengers), biphasic reaction systems or by playing with the calcination temperature of the catalyst, this problem can be diminished. In the case of the utilization of the layered structure as a catalyst in a batch reaction process, special attention should be given to the possible intercalation/stabilization of the reaction products in the interlayer space, which can affect catalyst reusability. In the case of using the mixed oxide catalyst in liquid phase reactions swelling of the clay-type material must also be taken into account. Hybrid materials can provide a solution.

Finally, the emerging literature reports and recent patents regarding biorefinery upgrading reactions with hydrotalcite materials show their commercial potential in this field.

Conflicts of interest

There are no conflicts of interest to declare.

References

1 G. W. Huber, J. N. Chheda, C. J. Barrett and J. A. Dumesic, Production of liquid alkanes by aqueous-phase processing of biomass-derived carbohydrates, *Science*, 2005, **308**, 1446–1450.

2 F. Cherubini, G. Jungmeier, M. Wellisch, T. Willke, I. Skiadas, R. Van Ree and E. de Jong, Toward a common

classification approach for biorefinery systems, *Biofuels, Bioprod. Biorefin.*, 2009, **3**, 534–546.
3 D. M. Alonso, J. Q. Bond and J. A. Dumesic, Catalytic conversion of biomass to biofuels, *Green Chem.*, 2010, **12**, 1493–1513.
4 J.-P. Mikkola, E. Sklavounos, A. W. T. King and P. Virtanen, *CHAPTER 1 The Biorefinery and Green Chemistry, Ionic Liquids in the Biorefinery Concept: Challenges and Perspectives*, The Royal Society of Chemistry, 2016, pp. 1–37.
5 V. Menon and M. Rao, Trends in bioconversion of lignocellulose: Biofuels, platform chemicals & biorefinery concept, *Prog. Energy Combust. Sci.*, 2012, **38**, 522–550.
6 H. Kobayashi and A. Fukuoka, Synthesis and utilisation of sugar compounds derived from lignocellulosic biomass, *Green Chem.*, 2013, **15**, 1740–1763.
7 L. D. Sousa, S. P. S. Chundawat, V. Balan and B. E. Dale, 'Cradle-to-grave' assessment of existing lignocellulose pretreatment technologies, *Curr. Opin. Biotechnol.*, 2009, **20**, 339–347.
8 P. Kumar, D. M. Barrett, M. J. Delwiche and P. Stroeve, Methods for Pretreatment of Lignocellulosic Biomass for Efficient Hydrolysis and Biofuel Production, *Ind. Eng. Chem. Res.*, 2009, **48**, 3713–3729.
9 C. J. Liu, H. M. Wang, A. M. Karim, J. M. Sun and Y. Wang, Catalytic fast pyrolysis of lignocellulosic biomass, *Chem. Soc. Rev.*, 2014, **43**, 7594–7623.
10 P. D. de Maria, P. M. Grande and W. Leitner, Current Trends in Pretreatment and Fractionation of Lignocellulose as Reflected in Industrial Patent Activities, *Chem. Ing. Tech.*, 2015, **87**, 1686–1695.
11 B. F. Sels, D. E. De Vos and P. A. Jacobs, Hydrotalcite-like anionic clays in catalytic organic reactions, *Catal. Rev.: Sci. Eng.*, 2001, **43**, 443–488.
12 G. Centi and S. Perathoner, Catalysis by layered materials: A review, *Microporous Mesoporous Mater.*, 2008, **107**, 3–15.
13 A. Primo and H. Garcia, Zeolites as catalysts in oil refining, *Chem. Soc. Rev.*, 2014, **43**, 7548–7561.
14 E. T. C. Vogt and B. M. Weckhuysen, Fluid catalytic cracking: recent developments on the grand old lady of zeolite catalysis, *Chem. Soc. Rev.*, 2015, **44**, 7342–7370.
15 S. Nishimura, A. Takagaki and K. Ebitani, Characterization, synthesis and catalysis of hydrotalcite-related materials for highly efficient materials transformations, *Green Chem.*, 2013, **15**, 2026–2042.
16 I. Delidovich, K. Leonhard and R. Palkovits, Cellulose and hemicellulose valorisation: an integrated challenge of catalysis and reaction engineering, *Energy Environ. Sci.*, 2014, **7**, 2803–2830.
17 D. Kubicka and O. Kikhtyanin, Opportunities for zeolites in biomass upgrading Lessons from the refining and petrochemical industry, *Catal. Today*, 2015, **243**, 10–22.
18 M. Hara, K. Nakajima and K. Kamata, Recent progress in the development of solid catalysts for biomass conversion into high value-added chemicals, *Sci. Technol. Adv. Mater.*, 2015, 16.
19 W. Wang, Z. Xu, Z. Guo, C. Jiang and W. Chu, Layered double hydroxide and related catalysts for hydrogen production and a biorefinery, *Chin. J. Catal.*, 2015, **36**, 139–147.
20 J. T. Feng, Y. F. He, Y. N. Liu, Y. Y. Du and D. Q. Li, Supported catalysts based on layered double hydroxides for catalytic oxidation and hydrogenation: general functionality and promising application prospects, *Chem. Soc. Rev.*, 2015, **44**, 5291–5319.
21 H. Li, Z. Fang, R. L. Smith and S. Yang, Efficient valorization of biomass to biofuels with bifunctional solid catalytic materials, *Prog. Energy Combust. Sci.*, 2016, **55**, 98–194.
22 T. Ennaert, J. Van Aelst, J. Dijkmans, R. De Clercq, W. Schutyser, M. Dusselier, D. Verboekend and B. F. Sels, Potential and challenges of zeolite chemistry in the catalytic conversion of biomass, *Chem. Soc. Rev.*, 2016, **45**, 584–611.
23 K. Yan, Y. Q. Liu, Y. R. Lu, J. J. Chai and L. P. Sun, Catalytic application of layered double hydroxide-derived catalysts for the conversion of biomass-dderived molecules, *Catal. Sci. Technol.*, 2017, **7**, 1622–1645.
24 F. Cavani, F. Trifiro and A. Vaccari, Hydrotalcite-type anionic clays: preparation, properties and applications, *Catal. Today*, 1991, **11**, 173–301.
25 A. I. Khan and D. O'Hare, Intercalation chemistry of layered double hydroxides: recent developments and applications, *J. Mater. Chem.*, 2002, **12**, 3191–3198.
26 D. G. Evans and R. C. T. Slade, Structural aspects of layered double hydroxides, in *Layered Double Hydroxides*, ed. X. Duan and D. G. Evans, 2006, pp. 1–87.
27 S. Kannan, Catalytic applications of hydrotalcite-like materials and their derived forms, *Catal. Surv. Asia*, 2006, **10**, 117–137.
28 D. P. Debecker, E. M. Gaigneaux and G. Busca, Exploring, Tuning, and Exploiting the Basicity of Hydrotalcites for Applications in Heterogeneous Catalysis, *Chem. – Eur. J.*, 2009, **15**, 3920–3935.
29 Z. P. Xu, J. Zhang, M. O. Adebajo, H. Zhang and C. Zhou, Catalytic applications of layered double hydroxides and derivatives, *Appl. Clay Sci.*, 2011, **53**, 139–150.
30 G. L. Fan, F. Li, D. G. Evans and X. Duan, Catalytic applications of layered double hydroxides: recent advances and perspectives, *Chem. Soc. Rev.*, 2014, **43**, 7040–7066.
31 R. Salomão, L. M. Milena, M. H. Wakamatsu and V. C. Pandolfelli, Hydrotalcite synthesis *via* co-precipitation reactions using MgO and Al(OH)3 precursors, *Ceram. Int.*, 2011, **37**, 3063–3070.
32 A. M. Fogg, A. L. Rohl, G. M. Parkinson and D. O'Hare, Predicting guest orientations in layered double hydroxide intercalates, *Chem. Mater.*, 1999, **11**, 1194–1200.
33 J. C. A. A. Roelofs, D. J. Lensveld, A. J. van Dillen and K. P. de Jong, On the Structure of Activated Hydrotalcites as Solid Base Catalysts for Liquid-Phase Aldol Condensation, *J. Catal.*, 2001, **203**, 184–191.
34 J.-T. Feng, Y.-J. Lin, D. G. Evans, X. Duan and D.-Q. Li, Enhanced metal dispersion and hydrodechlorination pro-

perties of a Ni/Al2O3 catalyst derived from layered double hydroxides, *J. Catal.*, 2009, **266**, 351–358.
35 S. Abello, F. Medina, D. Tichit, J. Perez-Ramirez, Y. Cesteros, P. Salagre and J. E. Sueiras, Nanoplatelet-based reconstructed hydrotalcites: towards more efficient solid base catalysts in aldol condensations, *Chem. Commun.*, 2005, 1453–1455.
36 S. Abello, F. Medina, D. Tichit, J. Perez-Ramirez, J. C. Groen, J. E. Sueiras, P. Salagre and Y. Cesteros, Aldol condensations over reconstructed Mg-Al hydrotalcites: Structure-activity relationships related to the rehydration method, *Chem. – Eur. J.*, 2005, **11**, 728–739.
37 J. Perez-Ramirez, S. Abello and N. M. van der Pers, Memory effect of activated Mg-Al hydrotalcite: In situ XRD studies during decomposition and gas-phase reconstruction, *Chem. – Eur. J.*, 2007, **13**, 870–878.
38 R. J. Chimentao, S. Abello, F. Medina, J. Llorca, J. E. Sueiras, Y. Cesteros and P. Salagre, Defect-induced strategies for the creation of highly active hydrotalcites in base-catalyzed reactions, *J. Catal.*, 2007, **252**, 249–257.
39 G. Lee, Y. Jeong, A. Takagaki and J. C. Jung, Sonication assisted rehydration of hydrotalcite catalyst for isomerization of glucose to fructose, *J. Mol. Catal. A: Chem.*, 2014, **393**, 289–295.
40 K. Takehira, Recent development of layered double hydroxide-derived catalysts - Rehydration, reconstitution, and supporting, aiming at commercial application, *Appl. Clay Sci.*, 2017, **136**, 112–141.
41 D. Tichit, D. Lutic, B. Coq, R. Durand and R. Teissier, The aldol condensation of acetaldehyde and heptanal on hydrotalcite-type catalysts, *J. Catal.*, 2003, **219**, 167–175.
42 D. Tichit, C. Gerardin, R. Durand and B. Coq, Layered double hydroxides: precursors for multifunctional catalysts, *Top. Catal.*, 2006, **39**, 89–96.
43 J. S. Valente, F. Figueras, M. Gravelle, P. Kumbhar, J. Lopez and J. P. Besse, Basic properties of the mixed oxides obtained by thermal decomposition of hydrotalcites containing different metallic compositions, *J. Catal.*, 2000, **189**, 370–381.
44 W. T. Reichle, Catalytic reactions by thermally activated, synthetic, anionic clay minerals, *J. Catal.*, 1985, **94**, 547–557.
45 O. D. Pavel, D. Tichit and I.-C. Marcu, Acido-basic and catalytic properties of transition-metal containing Mg–Al hydrotalcites and their corresponding mixed oxides, *Appl. Clay Sci.*, 2012, **61**, 52–58.
46 W. Y. Hernández, F. Aliç, A. Verberckmoes and P. Van Der Voort, Tuning the acidic–basic properties by Zn-substitution in Mg–Al hydrotalcites as optimal catalysts for the aldol condensation reaction, *J. Mater. Sci.*, 2017, **52**, 628–642.
47 A. Corma, V. Fornés, R. M. Martín-Aranda and F. Rey, Determination of base properties of hydrotalcites: Condensation of benzaldehyde with ethyl acetoacetate, *J. Catal.*, 1992, **134**, 58–65.
48 F. Prinetto, G. Ghiotti, R. Durand and D. Tichit, Investigation of Acid–Base Properties of Catalysts Obtained from Layered Double Hydroxides, *J. Phys. Chem. B*, 2000, **104**, 11117–11126.
49 J. S. Valente, H. Pfeiffer, E. Lima, J. Prince and J. Flores, Cyanoethylation of alcohols by activated Mg-Al layered double hydroxides: Influence of rehydration conditions and Mg/Al molar ratio on Bronsted basicity, *J. Catal.*, 2011, **279**, 196–204.
50 M. G. Alvarez, R. J. Chimentao, F. Figueras and F. Medina, Tunable basic and textural properties of hydrotalcite derived materials for transesterification of glycerol, *Appl. Clay Sci.*, 2012, **58**, 16–24.
51 M. Hajek, P. Kutalek, L. Smolakova, I. Troppova, L. Capek, D. Kubicka, J. Kocik and D. N. Thanh, Transesterification of rapeseed oil by Mg-Al mixed oxides with various Mg/Al molar ratio, *Chem. Eng. J.*, 2015, **263**, 160–167.
52 B. M. Choudary, S. Madhi, N. S. Chowdari, M. L. Kantam and B. Sreedhar, Layered double hydroxide supported nanopalladium catalyst for Heck-, Suzuki-, Sonogashira-, and Stille-type coupling reactions of chloroarenes, *J. Am. Chem. Soc.*, 2002, **124**, 14127–14136.
53 A. Mastalir and Z. Kiraly, Pd nanoparticles in hydrotalcite: mild and highly selective catalysts for alkyne semihydrogenation, *J. Catal.*, 2003, **220**, 372–381.
54 F. Prinetto, M. Manzoli, G. Ghiotti, M. D. M. Ortiz, D. Tichit and B. Coq, Pd/Mg(Al)O catalysts obtained from hydrotalcites: investigation of acid-base properties and nature of Pd phases, *J. Catal.*, 2004, **222**, 238–249.
55 P. J. Sideris, U. G. Nielsen, Z. H. Gan and C. P. Grey, Mg/Al ordering in layered double hydroxides revealed by multinuclear NMR spectroscopy, *Science*, 2008, **321**, 113–117.
56 P. J. Sideris, F. Blanc, Z. H. Gan and C. P. Grey, Identification of Cation Clustering in Mg-Al Layered Double Hydroxides Using Multinuclear Solid State Nuclear Magnetic Resonance Spectroscopy, *Chem. Mater.*, 2012, **24**, 2449–2461.
57 D. L. Carvalho, R. R. de Avillez, M. T. Rodrigues, L. E. P. Borges and L. G. Appel, Mg and Al mixed oxides and the synthesis of n-butanol from ethanol, *Appl. Catal., A*, 2012, **415**, 96–100.
58 A. I. Tsyganok, T. Tsunoda, S. Hamakawa, K. Suzuki, K. Takehira and T. Hayakawa, Dry reforming of methane over catalysts derived from nickel-containing Mg-Al layered double hydroxides, *J. Catal.*, 2003, **213**, 191–203.
59 L. Chmielarz, P. Kustrowski, A. Rafalska-Lasocha and R. Dziembaj, Influence of Cu, Co and Ni cations incorporated in brucite-type layers on thermal behaviour of hydrotalcites and reducibility of the derived mixed oxide systems, *Thermochim. Acta*, 2003, **395**, 225–236.
60 D. Tichit, M. D. M. Ortiz, D. Francova, C. Gerardin, B. Coq, R. Durand, F. Prinetto and G. Ghiotti, Design of nanostructured multifunctional Pd-based catalysts from layered double hydroxides precursors, *Appl. Catal., A*, 2007, **318**, 170–177.
61 C. Resini, T. Montanari, L. Barattini, G. Ramis, G. Busca, S. Presto, P. Riani, R. Marazza, M. Sisani, F. Marmottini and U. Costantino, Hydrogen production by ethanol

steam reforming over Ni catalysts derived from hydrotalcite-like precursors: Catalyst characterization, catalytic activity and reaction path, *Appl. Catal., A*, 2009, **355**, 83–93.

62 J. T. Feng, Y. J. Lin, D. G. Evans, X. Duan and D. Q. Li, Enhanced metal dispersion and hydrodechlorination properties of a Ni/Al2O3 catalyst derived from layered double hydroxides, *J. Catal.*, 2009, **266**, 351–358.

63 C. E. Daza, J. Gallego, F. Mondragon, S. Moreno and R. Molina, High stability of Ce-promoted Ni/Mg-Al catalysts derived from hydrotalcites in dry reforming of methane, *Fuel*, 2010, **89**, 592–603.

64 P. Gao, F. Li, H. J. Zhan, N. Zhao, F. K. Xiao, W. Wei, L. S. Zhong, H. Wang and Y. H. Sun, Influence of Zr on the performance of Cu/Zn/Al/Zr catalysts *via* hydrotalcite-like precursors for CO2 hydrogenation to methanol, *J. Catal.*, 2013, **298**, 51–60.

65 X. P. Yu, W. Chu, N. Wang and F. Ma, Hydrogen Production by Ethanol Steam Reforming on NiCuMgAl Catalysts Derived from Hydrotalcite-Like Precursors, *Catal. Lett.*, 2011, **141**, 1228–1236.

66 R. L. Manfro, T. Pires, N. F. P. Ribeiro and M. Souza, Aqueous-phase reforming of glycerol using Ni-Cu catalysts prepared from hydrotalcite-like precursors, *Catal. Sci. Technol.*, 2013, **3**, 1278–1287.

67 B. Dragoi, A. Ungureanu, A. Chirieac, C. Ciotonea, C. Rudolf, S. Royer and E. Dumitriu, Structural and catalytic properties of mono- and bimetallic nickel-copper nanoparticles derived from MgNi(Cu)Al-LDHs under reductive conditions, *Appl. Catal., A*, 2015, **504**, 92–102.

68 B. Coq, D. Tichit and S. Ribet, Co/Ni/Mg/Al layered double hydroxides as precursors of catalysts for the hydrogenation of nitriles: Hydrogenation of acetonitrile, *J. Catal.*, 2000, **189**, 117–128.

69 J. G. Zhang, H. Wang and A. K. Dalai, Development of stable bimetallic catalysts for carbon dioxide reforming of methane, *J. Catal.*, 2007, **249**, 300–310.

70 Y. Z. Yue, F. Liu, L. Zhao, L. H. Zhang and Y. Liu, Loading oxide nano sheet supported Ni-Co alloy nanoparticles on the macroporous walls of monolithic alumina and their catalytic performance for ethanol steam reforming, *Int. J. Hydrogen Energy*, 2015, **40**, 7052–7063.

71 S. X. Xia, Z. L. Yuan, L. N. Wang, P. Chen and Z. Y. Hou, Hydrogenolysis of glycerol on bimetallic Pd-Cu/solid-base catalysts prepared via layered double hydroxides precursors, *Appl. Catal., A*, 2011, **403**, 173–182.

72 Y. A. Liu, Y. F. He, D. R. Zhou, J. T. Feng and D. Q. Li, Catalytic performance of Pd-promoted Cu hydrotalcite-derived catalysts in partial hydrogenation of acetylene: effect of Pd-Cu alloy formation, *Catal. Sci. Technol.*, 2016, **6**, 3027–3037.

73 P. Beaudot, M. E. De Roy and J. P. Besse, Intercalation of noble metal complexes in LDH compounds, *J. Solid State Chem.*, 2004, **177**, 2691–2698.

74 C. Gerardin, D. Kostadinova, N. Sanson, B. Coq and D. Tichit, Supported metal particles from LDH nanocomposite precursors: Control of the metal particle size at increasing metal content, *Chem. Mater.*, 2005, **17**, 6473–6478.

75 A. Tsyganok and A. Sayari, Incorporation of transition metals into Mg–Al layered double hydroxides: Coprecipitation of cations *vs*. their pre-complexation with an anionic chelator, *J. Solid State Chem.*, 2006, **179**, 1830–1841.

76 T. Baskaran, J. Christopher and A. Sakthivel, Progress on layered hydrotalcite (HT) materials as potential support and catalytic materials, *RSC Adv.*, 2015, **5**, 98853–98875.

77 K. Takehira, Novel Preparation of Uniform Heterogeneous Catalysts Derived from Hydrotalcites, *J. Jpn. Pet. Inst.*, 2009, **52**, 145–158.

78 D. Li, K. Nishida, Y. Y. Zhan, T. Shishido, Y. Oumi, T. Sano and K. Takehira, Superior catalytic behavior of trace Pt-doped Ni/Mg(Al)O in methane reforming under daily start-up and shut-down operation, *Appl. Catal., A*, 2008, **350**, 225–236.

79 M. J. Climent, A. Corma, S. Iborra and M. J. Sabater, Heterogeneous Catalysis for Tandem Reactions, *ACS Catal.*, 2014, **4**, 870–891.

80 G. D. Yadav and P. Aduri, Aldol condensation of benzaldehyde with heptanal to jasminaldehyde over novel Mg-Al mixed oxide on hexagonal mesoporous silica, *J. Mol. Catal. A: Chem.*, 2012, **355**, 142–154.

81 W. Y. Hernández, K. De Vlieger, P. Van Der Voort and A. Verberckmoes, Ni–Cu Hydrotalcite-Derived Mixed Oxides as Highly Selective and Stable Catalysts for the Synthesis of β-Branched Bioalcohols by the Guerbet Reaction, *ChemSusChem*, 2016, **9**, 3196–3205.

82 A. A. Rosatella, S. P. Simeonov, R. F. M. Frade and C. A. M. Afonso, 5-Hydroxymethylfurfural (HMF) as a building block platform: Biological properties, synthesis and synthetic applications, *Green Chem.*, 2011, **13**, 754–793.

83 H. Tumturk, G. Demirel, H. Altinok, S. Aksoy and N. Hasirci, Immobilization of glucose isomerase in surface-modified alginate gel beads, *J. Food Biochem.*, 2008, **32**, 234–246.

84 D. H. Yu, H. Wu, A. J. Zhang, L. Tian, L. D. Liu, C. M. Wang and X. X. Fang, Microwave irradiation-assisted isomerization of glucose to fructose by immobilized glucose isomerase, *Process Biochem.*, 2011, **46**, 599–603.

85 I. Delidovich and R. Palkovits, Catalytic Isomerization of Biomass-Derived Aldoses: A Review, *ChemSusChem*, 2016, **9**, 547–561.

86 C. Kooyman, K. Vellenga and H. G. J. Dewilt, Isomerization of d-glucose into d-fructose in aqueous alkaline-solutions, *Carbohydr. Res.*, 1977, **54**, 33–44.

87 M. Watanabe, Y. Aizawa, T. Iida, T. M. Aida, C. Levy, K. Sue and H. Inomata, Glucose reactions with acid and base catalysts in hot compressed water at 473 K, *Carbohydr. Res.*, 2005, **340**, 1925–1930.

88 C. Moreau, R. Durand, A. Roux and D. Tichit, Isomerization of glucose into fructose in the presence of

cation-exchanged zeolites and hydrotalcites, *Appl. Catal., A*, 2000, **193**, 257–264.
89 J. Lecomte, A. Finiels and C. Moreau, Kinetic study of the isomerization of glucose into fructose in the presence of anion-modified hydrotalcites, *Starch/Stärke*, 2002, **54**, 75–79.
90 S. Yu, E. Kim, S. Park, I. K. Song and J. C. Jung, Isomerization of glucose into fructose over Mg–Al hydrotalcite catalysts, *Catal. Commun.*, 2012, **29**, 63–67.
91 Q. Yang, S. Zhou and T. Runge, Magnetically separable base catalysts for isomerization of glucose to fructose, *J. Catal.*, 2015, **330**, 474–484.
92 M. Moliner, Y. Roman-Leshkov and M. E. Davis, Tin-containing zeolites are highly active catalysts for the isomerization of glucose in water, *Proc. Natl. Acad. Sci. U. S. A.*, 2010, **107**, 6164–6168.
93 I. Delidovich and R. Palkovits, Catalytic activity and stability of hydrophobic Mg-Al hydrotalcites in the continuous aqueous-phase isomerization of glucose into fructose, *Catal. Sci. Technol.*, 2014, **4**, 4322–4329.
94 I. Delidovich and R. Palkovits, Structure-performance correlations of Mg-Al hydrotalcite catalysts for the isomerization of glucose into fructose, *J. Catal.*, 2015, **327**, 1–9.
95 Chemical method for catalyzing glucose into fructose through isomerization, CN 104262416 A, 2015.
96 A. Takagaki, M. Ohara, S. Nishimura and K. Ebitani, A one-pot reaction for biorefinery: combination of solid acid and base catalysts for direct production of 5-hydroxymethylfurfural from saccharides, *Chem. Commun.*, 2009, 6276–6278.
97 A. Takagaki, M. Takahashi, S. Nishimura and K. Ebitani, One-Pot Synthesis of 2,5-Diformylfuran from Carbohydrate Derivatives by Sulfonated Resin and Hydrotalcite-Supported Ruthenium Catalysts, *ACS Catal.*, 2011, **1**, 1562–1565.
98 J. Tuteja, S. Nishimura and K. Ebitani, One-Pot Synthesis of Furans from Various Saccharides Using a Combination of Solid Acid and Base Catalysts, *Bull. Chem. Soc. Jpn.*, 2012, **85**, 275–281.
99 M. Shirotori, S. Nishimura and K. Ebitani, One-pot synthesis of furfural derivatives from pentoses using solid acid and base catalysts, *Catal. Sci. Technol.*, 2014, **4**, 971–978.
100 M. Shirotori, S. Nishimura and K. Ebitani, One-pot Synthesis of Furfural from Xylose using Al2O3-Ni-Al Layered Double Hydroxide Acid-Base Bi-functional Catalyst and Sulfonated Resin, *Chem. Lett.*, 2016, **45**, 194–196.
101 K. Ebitani, A. Takagaki and 高垣敦, Method for preparing 5-hydroxymethylfurfural, WO 2010101024 A1, 2010.
102 K. Yan, G. Wu, T. Lafleur and C. Jarvis, Production, properties and catalytic hydrogenation of furfural to fuel additives and value-added chemicals, *Renewable Sustainable Energy Rev.*, 2014, **38**, 663–676.
103 Y. Nakagawa, M. Tamura and K. Tomishige, Catalytic Reduction of Biomass-Derived Furanic Compounds with Hydrogen, *ACS Catal.*, 2013, **3**, 2655–2668.
104 C. P. Jiménez-Gómez, J. A. Cecilia, D. Durán-Martín, R. Moreno-Tost, J. Santamaría-González, J. Mérida-Robles, R. Mariscal and P. Maireles-Torres, Gas-phase hydrogenation of furfural to furfuryl alcohol over Cu/ZnO catalysts, *J. Catal.*, 2016, **336**, 107–115.
105 M. M. Villaverde, N. M. Bertero, T. F. Garetto and A. J. Marchi, Selective liquid-phase hydrogenation of furfural to furfuryl alcohol over Cu-based catalysts, *Catal. Today*, 2013, **213**, 87–92.
106 Y. Wang, M. H. Zhou, T. Z. Wang and G. M. Xiao, Conversion of Furfural to Cyclopentanol on Cu/Zn/Al Catalysts Derived from Hydrotalcite-Like Materials, *Catal. Lett.*, 2015, **145**, 1557–1565.
107 M. Manikandan, A. K. Venugopal, K. Prabu, R. K. Jha and R. Thirumalaiswamy, Role of surface synergistic effect on the performance of Ni-based hydrotalcite catalyst for highly efficient hydrogenation of furfural, *J. Mol. Catal. A: Chem.*, 2016, **417**, 153–162.
108 Y. Nakagawa, H. Nakazawa, H. Watanabe and K. Tomishige, Total Hydrogenation of Furfural over a Silica-Supported Nickel Catalyst Prepared by the Reduction of a Nickel Nitrate Precursor, *ChemCatChem*, 2012, **4**, 1791–1797.
109 R. Thirumalaiswamy, M. Marimuthu and K. V. Ashok, Ni containing anionic clay catalyst useful for selective hydrogenation of furfural to furfuryl alcohol and its preparation thereof, WO 2015198351 A2, 2015.
110 T. Mizugaki, T. Yamakawa, Y. Nagatsu, Z. Maeno, T. Mitsudome, K. Jitsukawa and K. Kaneda, Direct Transformation of Furfural to 1,2-Pentanediol Using a Hydrotalcite-Supported Platinum Nanoparticle Catalyst, *ACS Sustainable Chem. Eng.*, 2014, **2**, 2243–2247.
111 C. H. Xu, L. K. Zheng, D. F. Deng, J. Y. Liu and S. Y. Liu, Effect of activation temperature on the surface copper particles and catalytic properties of Cu-Ni-Mg-Al oxides from hydrotalcite-like precursors, *Catal. Commun.*, 2011, **12**, 996–999.
112 C. H. Xu, L. K. Zheng, J. Y. Liu and Z. Y. Huang, Furfural Hydrogenation on Nickel-promoted Cu-containing Catalysts Prepared from Hydrotalcite-Like Precursors, *Chin. J. Chem.*, 2011, **29**, 691–697.
113 H. Y. Zhu, M. H. Zhou, Z. Zeng, G. M. Xiao and R. Xiao, Selective hydrogenation of furfural to cyclopentanone over Cu-Ni-Al hydrotalcite-based catalysts, *Korean J. Chem. Eng.*, 2014, **31**, 593–597.
114 C. M. Li, Y. D. Chen, S. T. Zhang, S. M. Xu, J. Y. Zhou, F. Wang, M. Wei, D. G. Evans and X. Duan, Ni-In Intermetallic Nanocrystals as Efficient Catalysts toward Unsaturated Aldehydes Hydrogenation, *Chem. Mater.*, 2013, **25**, 3888–3896.
115 F. M. Ren, Z. Wang, L. F. Luo, H. Y. Lu, G. Zhou, W. X. Huang, X. Hong, Y. E. Wu and Y. D. Li, Utilization of Active Ni to Fabricate Pt-Ni Nanoframe/NiAl Layered Double Hydroxide Multifunctional Catalyst through In Situ Precipitation, *Chem. – Eur. J.*, 2015, **21**, 13181–13185.

116 K. Yan and A. Chen, Efficient hydrogenation of biomass-derived furfural and levulinic acid on the facilely synthesized noble-metal-free Cu–Cr catalyst, *Energy*, 2013, **58**, 357–363.

117 M. Lesiak, M. Binczarski, S. Karski, W. Maniukiewicz, J. Rogowski, E. Szubiakiewicz, J. Berlowska, P. Dziugan and I. Witońska, Hydrogenation of furfural over Pd–Cu/Al2O3 catalysts. The role of interaction between palladium and copper on determining catalytic properties, *J. Mol. Catal. A: Chem.*, 2014, **395**, 337–348.

118 M. Pierre, Method for the catalytic hydrogenation of furfural, US 2763666 A, 1956.

119 Á. O'Driscoll, T. Curtin, W. Y. Hernández, P. Van Der Voort and J. J. Leahy, Hydrogenation of Furfural with a Pt–Sn Catalyst: The Suitability to Sustainable Industrial Application, *Org. Process Res. Dev.*, 2016, **20**, 1917–1929.

120 C. J. Barrett, J. N. Chheda, G. W. Huber and J. A. Dumesic, Single-reactor process for sequential aldol-condensation and hydrogenation of biomass-derived compounds in water, *Appl. Catal., B*, 2006, **66**, 111–118.

121 H. Liu, W. Xu, X. Liu, Y. Guo, Y. Guo, G. Lu and Y. Wang, Aldol condensation of furfural and acetone on layered double hydroxides, *Kinet. Catal.*, 2010, **51**, 75–80.

122 W. Xu, X. Liu, J. Ren, P. Zhang, Y. Wang, Y. Guo, Y. Guo and G. Lu, A novel mesoporous Pd/cobalt aluminate bifunctional catalyst for aldol condensation and following hydrogenation, *Catal. Commun.*, 2010, **11**, 721–726.

123 S. Ordóñez, E. Díaz, M. León and L. Faba, Hydrotalcite-derived mixed oxides as catalysts for different C–C bond formation reactions from bioorganic materials, *Catal. Today*, 2011, **167**, 71–76.

124 L. Hora, V. Kelbichová, O. Kikhtyanin, O. Bortnovskiy and D. Kubička, Aldol condensation of furfural and acetone over MgAl layered double hydroxides and mixed oxides, *Catal. Today*, 2014, **223**, 138–147.

125 L. Hora, O. Kikhtyanin, L. Čapek, O. Bortnovskiy and D. Kubička, Comparative study of physico-chemical properties of laboratory and industrially prepared layered double hydroxides and their behavior in aldol condensation of furfural and acetone, *Catal. Today*, 2015, **241**(Part B), 221–230.

126 O. Kikhtyanin, V. Kelbichova, D. Vitvarova, M. Kubu and D. Kubicka, Aldol condensation of furfural and acetone on zeolites, *Catal. Today*, 2014, **227**, 154–162.

127 L. Faba, E. Diaz and S. Ordonez, Aqueous-phase furfural-acetone aldol condensation over basic mixed oxides, *Appl. Catal., B*, 2012, **113**, 201–211.

128 Z. Zhang and K. Deng, Recent Advances in the Catalytic Synthesis of 2,5-Furandicarboxylic Acid and Its Derivatives, *ACS Catal.*, 2015, **5**, 6529–6544.

129 A. Gandini, A. J. D. Silvestre, C. P. Neto, A. F. Sousa and M. Gomes, The furan counterpart of poly(ethylene terephthalate): An alternative material based on renewable resources, *J. Polym. Sci., Part A: Polym. Chem.*, 2009, **47**, 295–298.

130 A. Gandini, Furans as offspring of sugars and polysaccharides and progenitors of a family of remarkable polymers: a review of recent progress, *Polym. Chem.*, 2010, **1**, 245–251.

131 N. Dimitratos, A. Villa, C. L. Bianchi, L. Prati and M. Makkee, Gold on titania: Effect of preparation method in the liquid phase oxidation, *Appl. Catal., A*, 2006, **311**, 185–192.

132 J. Zhu, J. L. Figueiredo and J. L. Faria, Au/activated-carbon catalysts for selective oxidation of alcohols with molecular oxygen under atmospheric pressure: Role of basicity, *Catal. Commun.*, 2008, **9**, 2395–2397.

133 N. K. Gupta, S. Nishimura, A. Takagaki and K. Ebitani, Hydrotalcite-supported gold-nanoparticle-catalyzed highly efficient base-free aqueous oxidation of 5-hydroxymethylfurfural into 2,5-furandicarboxylic acid under atmospheric oxygen pressure, *Green Chem.*, 2011, **13**, 824–827.

134 B. N. Zope, S. E. Davis and R. J. Davis, Influence of Reaction Conditions on Diacid Formation During Au-Catalyzed Oxidation of Glycerol and Hydroxymethylfurfural, *Top. Catal.*, 2012, **55**, 24–32.

135 G. Yi and Y. Zhang, Conversion and purification of biomass, US 20160207899 A1, 2016.

136 L. Ardemani, G. Cibin, A. J. Dent, M. A. Isaacs, G. Kyriakou, A. F. Lee, C. M. A. Parlett, S. A. Parry and K. Wilson, Solid base catalysed 5-HMF oxidation to 2,5-FDCA over Au/hydrotalcites: fact or fiction?, *Chem. Sci.*, 2015, **6**, 4940–4945.

137 H. Choudhary and K. Ebitani, Hydrotalcite-supported PdPt-catalyzed Aerobic Oxidation of 5-Hydroxymethylfurfural to 2,5-Furandicarboxylic Acid in Water, *Chem. Lett.*, 2016, **45**, 613–615.

138 M. J. Climent, A. Corma and S. Iborra, Conversion of biomass platform molecules into fuel additives and liquid hydrocarbon fuels, *Green Chem.*, 2014, **16**, 516–547.

139 M. Besson, P. Gallezot and C. Pinel, Conversion of Biomass into Chemicals over Metal Catalysts, *Chem. Rev.*, 2014, **114**, 1827–1870.

140 J. S. Luterbacher, J. M. Rand, D. M. Alonso, J. Han, J. T. Youngquist, C. T. Maravelias, B. F. Pfleger and J. A. Dumesic, Nonenzymatic Sugar Production from Biomass Using Biomass-Derived γ-Valerolactone, *Science*, 2014, **343**, 277–280.

141 X. Tang, X. Zeng, Z. Li, L. Hu, Y. Sun, S. Liu, T. Lei and L. Lin, Production of γ-valerolactone from lignocellulosic biomass for sustainable fuels and chemicals supply, *Renewable Sustainable Energy Rev.*, 2014, **40**, 608–620.

142 K. Yan and A. C. Chen, Efficient hydrogenation of biomass-derived furfural and levulinic acid on the facilely synthesized noble-metal-free Cu-Cr catalyst, *Energy*, 2013, **58**, 357–363.

143 K. Yan, J. Y. Liao, X. Wu and X. M. Xie, A noble-metal free Cu-catalyst derived from hydrotalcite for highly efficient hydrogenation of biomass-derived furfural and levulinic acid, *RSC Adv.*, 2013, **3**, 3853–3856.

144 W. Li, G. Fan, L. Yang and F. Li, Highly Efficient Vapor-Phase Hydrogenation of Biomass-Derived Levulinic Acid

Over Structured Nanowall-Like Nickel-Based Catalyst, *ChemCatChem*, 2016, **8**, 2724–2733.

145 Q. Hu, L. Yang, G. Fan and F. Li, Hydrogenation of biomass-derived compounds containing a carbonyl group over a copper-based nanocatalyst: Insight into the origin and influence of surface oxygen vacancies, *J. Catal.*, 2016, **340**, 184–195.

146 K. Srinivasan and S. Gundekari, A process for the preparation of gamma-valerolactone by catalytic hydrogenation of levulinic acid using ru-based catalysts, WO 2016056030 A1, 2016.

147 A. M. Hengne and C. V. Rode, Cu-ZrO2 nanocomposite catalyst for selective hydrogenation of levulinic acid and its ester to [gamma]-valerolactone, *Green Chem.*, 2012, **14**, 1064–1072.

148 M. Varkolu, V. Velpula, D. R. Burri and S. R. R. Kamaraju, Gas phase hydrogenation of levulinic acid to [gamma]-valerolactone over supported Ni catalysts with formic acid as hydrogen source, *New J. Chem.*, 2016, **40**, 3261–3267.

149 M. G. Al-Shaal, W. R. H. Wright and R. Palkovits, Exploring the ruthenium catalysed synthesis of [gamma]-valerolactone in alcohols and utilisation of mild solvent-free reaction conditions, *Green Chem.*, 2012, **14**, 1260–1263.

150 A. S. AlRamadan, S. M. Sarathy, M. Khurshid and J. Badra, A blending rule for octane numbers of PRFs and TPRFs with ethanol, *Fuel*, 2016, **180**, 175–186.

151 V. R. Surisetty, A. K. Dalai and J. Kozinski, Alcohols as alternative fuels: An overview, *Appl. Catal., A*, 2011, **404**, 1–11.

152 J. Sun and Y. Wang, Recent Advances in Catalytic Conversion of Ethanol to Chemicals, *ACS Catal.*, 2014, **4**, 1078–1090.

153 G. Nahar and V. Dupont, Hydrogen production from simple alkanes and oxygenated hydrocarbons over ceria-zirconia supported catalysts: Review, *Renewable Sustainable Energy Rev.*, 2014, **32**, 777–796.

154 S. Ahmed and M. Krumpelt, Hydrogen from hydrocarbon fuels for fuel cells, *Int. J. Hydrogen Energy*, 2001, **26**, 291–301.

155 C. Pirez, W. H. Fang, M. Capron, S. Paul, H. Jobic, F. Dumeignil and L. Jalowiecki-Duhamel, Steam reforming, partial oxidation and oxidative steam reforming for hydrogen production from ethanol over cerium nickel based oxyhydride catalyst, *Appl. Catal., A*, 2016, **518**, 78–86.

156 L. J. I. Coleman, W. Epling, R. R. Hudgins and E. Croiset, Ni/Mg-Al mixed oxide catalyst for the steam reforming of ethanol, *Appl. Catal., A*, 2009, **363**, 52–63.

157 S. Liu, D. Chen, K. Zhang, J. J. Li and N. Q. Zhao, Production of hydrogen by ethanol steam reforming over catalysts from reverse microemulsion-derived nanocompounds, *Int. J. Hydrogen Energy*, 2008, **33**, 3736–3747.

158 S. Velu, K. Suzuki, M. Vijayaraj, S. Barman and C. S. Gopinath, In situ XPS investigations of Cu1-xNixZnAl-mixed metal oxide catalysts used in the oxidative steam reforming of bio-ethanol, *Appl. Catal., B*, 2005, **55**, 287–299.

159 L. He, H. Berntsen, E. Ochoa-Fernandez, J. C. Walmsley, E. A. Blekkan and D. Chen, Co-Ni Catalysts Derived from Hydrotalcite-Like Materials for Hydrogen Production by Ethanol Steam Reforming, *Top. Catal.*, 2009, **52**, 206–217.

160 A. Romero, M. Jobbagy, M. Laborde, G. Baronetti and N. Amadeo, Ni(II)-Mg(II)-Al(III) catalysts for hydrogen production from ethanol steam reforming: Influence of the activation treatments, *Catal. Today*, 2010, **149**, 407–412.

161 M. S. Li, X. D. Wang, S. R. Li, S. P. Wang and X. B. Ma, Hydrogen production from ethanol steam reforming over nickel based catalyst derived from Ni/Mg/Al hydrotalcite-like compounds, *Int. J. Hydrogen Energy*, 2010, **35**, 6699–6708.

162 J. Bussi, M. Musso, S. Veiga, N. Bespalko, R. Faccio and A. C. Roger, Ethanol steam reforming over NiLaZr and NiCuLaZr mixed metal oxide catalysts, *Catal. Today*, 2013, **213**, 42–49.

163 R. Espinal, E. Taboada, E. Molins, R. J. Chimentao, F. Medina and J. Llorca, Cobalt hydrotalcites as catalysts for bioethanol steam reforming. The promoting effect of potassium on catalyst activity and long-term stability, *Appl. Catal., B*, 2012, **127**, 59–67.

164 A. A. Khassin, T. M. Yurieva, V. V. Kaichev, V. I. Bukhtiyarov, A. A. Budneva, E. A. Paukshtis and V. N. Parmon, Metal-support interactions in cobalt-aluminum co-precipitated catalysts: XPS and CO adsorption studies, *J. Mol. Catal. A: Chem.*, 2001, **175**, 189–204.

165 Y. Y. Liu, K. Murata and M. Inaba, Steam Reforming of Bio-Ethanol to Produce Hydrogen over Co/CeO2 Catalysts Derived from Ce1-xCoxO2-y Precursors, *Catalysts*, 2016, **6**, 14.

166 G. Brieger and T. J. Nestrick, Catalytic transfer hydrogenation, *Chem. Rev.*, 1974, **74**, 567–580.

167 G. Guillena, D. J. Ramon and M. Yus, Alcohols as electrophiles in C-C bond-forming reactions: The hydrogen autotransfer process, *Angew. Chem., Int. Ed.*, 2007, **46**, 2358–2364.

168 J. M. Hidalgo, C. Jimenez-Sanchidrian and J. R. Ruiz, Delaminated layered double hydroxides as catalysts for the Meerwein-Ponndorf-Verley reaction, *Appl. Catal., A*, 2014, **470**, 311–317.

169 R. Grigg, T. R. B. Mitchell and S. Sutthivaiyakit, Oxidation of alcohols by transition-metal complexes .4. the rhodium catalyzed synthesis of esters from aldehydes and alcohols, *Tetrahedron*, 1981, **37**, 4313–4319.

170 R. Grigg, T. R. B. Mitchell, S. Sutthivaiyakit and N. Tongpenyai, Oxidation of alcohols by transition-metal complexes .5. selective catalytic monoalkylation of arylacetonitriles by alcohols, *Tetrahedron Lett.*, 1981, **22**, 4107–4110.

171 C. S. Cho, B. T. Kim, T. J. Kim and S. C. Shim, An unusual type of ruthenium-catalyzed transfer hydrogenation of ketones with alcohols accompanied by C-C coupling, *J. Org. Chem.*, 2001, **66**, 9020–9022.

172 C. S. Cho, B. T. Kim, T. J. Kim and S. C. Shim, Ruthenium-catalyzed regioselective alpha-alkylation of ketones with primary alcohols, *Tetrahedron Lett.*, 2002, **43**, 7987–7989.

173 M. G. Edwards and J. M. J. Williams, Catalytic electronic activation: Indirect "Wittig" reaction of alcohols, *Angew. Chem., Int. Ed.*, 2002, **41**, 4740–4743.

174 K. Taguchi, H. Nakagawa, T. Hirabayashi, S. Sakaguchi and Y. Ishii, An efficient direct alpha-alkylation of ketones with primary alcohols catalyzed by Ir(cod)Cl (2)/PPh3/KOH system without solvent, *J. Am. Chem. Soc.*, 2004, **126**, 72–73.

175 R. Martinez, G. J. Brand, D. J. Ramon and M. Yus, Ru(DMSO)(4) Cl-2 catalyzes the alpha-alkylation of ketones by alcohols, *Tetrahedron Lett.*, 2005, **46**, 3683–3686.

176 G. R. A. Adair and J. M. J. Williams, Oxidant-free oxidation: ruthenium catalysed dehydrogenation of alcohols, *Tetrahedron Lett.*, 2005, **46**, 8233–8235.

177 K. Fujita, C. Asai, T. Yamaguchi, F. Hanasaka and R. Yamaguchi, Direct beta-alkylation of secondary alcohols with primary alcohols catalyzed by a Cp*lr complex, *Org. Lett.*, 2005, **7**, 4017–4019.

178 R. Martinez, D. J. Ramon and M. Yus, Easy alpha-alkylation of ketones with alcohols through a hydrogen autotransfer process catalyzed by RuCl2(DMSO)(4), *Tetrahedron*, 2006, **62**, 8988–9001.

179 R. Martinez, D. J. Ramon and M. Yus, RuCl2(DMSO)(4) catalyzes the beta-alkylation of secondary alcohols with primary alcohols through a hydrogen autotransfer process, *Tetrahedron*, 2006, **62**, 8982–8987.

180 C. S. Cho and S. C. Shim, A ruthenium-catalyzed one-pot method for alpha-alkylation of ketones with aldehydes, *J. Organomet. Chem.*, 2006, **691**, 4329–4332.

181 G. Onodera, Y. Nishibayashi and S. Uemura, Ir- and Ru-catalyzed sequential reactions: Asymmetric alpha-alkylative reduction of ketones with alcohols, *Angew. Chem., Int. Ed.*, 2006, **45**, 3819–3822.

182 P. J. Black, G. Cami-Kobeci, M. G. Edwards, P. A. Slatford, M. K. Whittlesey and J. M. J. Williams, Borrowing hydrogen: iridium-catalysed reactions for the formation of C-C bonds from alcohols, *Org. Biomol. Chem.*, 2006, **4**, 116–125.

183 P. A. Slatford, M. K. Whittlesey and J. M. J. Williams, C-C Bond formation from alcohols using a Xantphos ruthenium complex, *Tetrahedron Lett.*, 2006, **47**, 6787–6789.

184 K. Koda, T. Matsu-Ura, Y. Obora and Y. Ishii, Guerbet Reaction of Ethanol to n-Butanol Catalyzed by Iridium Complexes, *Chem. Lett.*, 2009, **38**, 838–839.

185 N. Yamamoto, Y. Obora and Y. Ishii, The Direct Conversion of Ethanol to Ethyl and Methyl Acetates Catalyzed by Iridium Complex, *Chem. Lett.*, 2009, **38**, 1106–1107.

186 G. R. M. Dowson, M. F. Haddow, J. Lee, R. L. Wingad and D. F. Wass, Catalytic Conversion of Ethanol into an Advanced Biofuel: Unprecedented Selectivity for n-Butanol, *Angew. Chem., Int. Ed.*, 2013, **52**, 9005–9008.

187 G. Q. Xu, T. Lammens, Q. Liu, X. C. Wang, L. L. Dong, A. Caiazzo, N. Ashraf, J. Guan and X. D. Mu, Direct self-condensation of bio-alcohols in the aqueous phase, *Green Chem.*, 2014, **16**, 3971–3977.

188 R. L. Wingad, P. J. Gates, S. T. G. Street and D. F. Wass, Catalytic Conversion of Ethanol to n-Butanol Using Ruthenium P-N Ligand Complexes, *ACS Catal.*, 2015, **5**, 5822–5826.

189 S. Chakraborty, P. E. Piszel, C. E. Hayes, R. T. Baker and W. D. Jones, Highly Selective Formation of n-Butanol from Ethanol through the Guerbet Process: A Tandem Catalytic Approach, *J. Am. Chem. Soc.*, 2015, **137**, 14264–14267.

190 R. L. Wingad, E. J. E. Bergstrom, M. Everett, K. J. Pellow and D. F. Wass, Catalytic conversion of methanol/ethanol to isobutanol - a highly selective route to an advanced biofuel, *Chem. Commun.*, 2016, **52**, 5202–5204.

191 Y. J. Xie, Y. Ben-David, L. J. W. Shimon and D. Milstein, Highly Efficient Process for Production of Biofuel from Ethanol Catalyzed by Ruthenium Pincer Complexes, *J. Am. Chem. Soc.*, 2016, **138**, 9077–9080.

192 W. M. Quattlebaum, W. J. Toussaint and J. T. Dunn, Deoxygenation of Certain Aldehydes and Ketones: Preparation of Butadiene and Styrene, *J. Am. Chem. Soc.*, 1947, **69**, 593–599.

193 T. Raja, T. M. Jyothi, K. Sreekumar, M. B. Talawar, J. Santhanalakshmi and B. S. Rao, Calcined layered double hydroxides as basic heterogeneous catalysts for the Oppenauer oxidation of alcohols, *Bull. Chem. Soc. Jpn.*, 1999, **72**, 2117–2119.

194 T. M. Jyothi, T. Raja, K. Sreekumar, M. B. Talawar and B. S. Rao, Influence of acid-base properties of mixed oxides derived from hydrotalcite-like precursors in the transfer hydrogenation of propiophenone, *J. Mol. Catal. A: Chem.*, 2000, **157**, 193–198.

195 M. A. Aramendía, V. Borau, C. Jimenez, J. M. Marinas, J. R. Ruiz and F. J. Urbano, Activity of basic catalysts in the Meerwein-Ponndorf-Verley reaction of benzaldehyde with ethanol, *J. Colloid Interface Sci.*, 2001, **238**, 385–389.

196 G. Onyestyák, G. Novodarszki, R. Barthos, S. Klebert, A. F. Wellisch and A. Pilbath, Acetone alkylation with ethanol over multifunctional catalysts by a borrowing hydrogen strategy, *RSC Adv.*, 2015, **5**, 99502–99509.

197 K. Motokura, D. Nishimura, K. Mori, T. Mizugaki, K. Ebitani and K. Kaneda, A ruthenium-grafted hydrotalcite as a multifunctional catalyst for direct alpha-alkylation of nitriles with primary alcohols, *J. Am. Chem. Soc.*, 2004, **126**, 5662–5663.

198 M. Dixit, M. Mishra, P. A. Joshi and D. O. Shah, Clean borrowing hydrogen methodology using hydrotalcite supported copper catalyst, *Catal. Commun.*, 2013, **33**, 80–83.

199 M. W. Farrar, US 2971033 A, 1961.

200 G. Pregaglia, G. Gregorio and F. Conti, *French Pat.*, 1531261, 1968.

201 R. T. Clark, US 3972952 A, 1976.

202 J. T. Kozlowski and R. J. Davis, Heterogeneous Catalysts for the Guerbet Coupling of Alcohols, *ACS Catal.*, 2013, **3**, 1588–1600.
203 D. Gabriels, W. Y. Hernandez, B. Sels, P. Van Der Voort and A. Verberckmoes, Review of catalytic systems and thermodynamics for the Guerbet condensation reaction and challenges for biomass valorization, *Catal. Sci. Technol.*, 2015, **5**, 3876–3902.
204 W. Ueda, T. Kuwabara, T. Ohshida and Y. Morikawa, A low-pressure guerbet reaction over magnesium-oxide catalyst, *J. Chem. Soc., Chem. Commun.*, 1990, 1558–1559.
205 A. S. Ndou, N. Plint and N. J. Coville, Dimerisation of ethanol to butanol over solid-base catalysts, *Appl. Catal., A*, 2003, **251**, 337–345.
206 C. Yang and Z. Y. Meng, Bimolecular condensation of ethanol to 1-butanol catalyzed by alkali cation zeolites, *J. Catal.*, 1993, **142**, 37–44.
207 I. C. Marcu, D. Tichit, F. Fajula and N. Tanchoux, Catalytic valorization of bioethanol over Cu-Mg-Al mixed oxide catalysts, *Catal. Today*, 2009, **147**, 231–238.
208 M. León, E. Díaz, S. Bennici, A. Vega, S. Ordónez and A. Auroux, Consequences of the iron-aluminium exchange on the performance of hydrotalcite-derived mixed oxides for ethanol condensation, *Appl. Catal., B*, 2011, **102**, 590–599.
209 M. León, E. Díaz and S. Ordónez, Ethanol catalytic condensation over Mg-Al mixed oxides derived from hydrotalcites, *Catal. Today*, 2011, **164**, 436–442.
210 T. Riittonen, E. Toukoniitty, D. K. Madnani, A. R. Leino, K. Kordas, M. Szabo, A. Sapi, K. Arve, J. Warna and J. P. Mikkola, One-Pot Liquid-Phase Catalytic Conversion of Ethanol to 1-Butanol over Aluminium Oxide-The Effect of the Active Metal on the Selectivity, *Catalysts*, 2012, **2**, 68–84.
211 J. J. Bravo-Suárez, B. Subramaniam and R. V. Chaudhari, Vapor-phase methanol and ethanol coupling reactions on CuMgAl mixed metal oxides, *Appl. Catal., A*, 2013, **455**, 234–246.
212 K. Shimura, K. Kon, S. M. A. Hakim Siddiki and K.-I. Shimizu, Self-coupling of secondary alcohols by Ni/CeO2 catalyst, *Appl. Catal., A*, 2013, **462–463**, 137–142.
213 I.-C. Marcu, N. Tanchoux, F. Fajula and D. Tichit, Catalytic Conversion of Ethanol into Butanol over M–Mg–Al Mixed Oxide Catalysts (M = Pd, Ag, Mn, Fe, Cu, Sm, Yb) Obtained from LDH Precursors, *Catal. Lett.*, 2013, **143**, 23–30.
214 T. Riittonen, K. Eränen, P. Mäki-Arvela, A. Shchukarev, A.-R. Rautio, K. Kordas, N. Kumar, T. Salmi and J.-P. Mikkola, Continuous liquid-phase valorization of bioethanol towards bio-butanol over metal modified alumina, *Renewable Energy*, 2015, **74**, 369–378.
215 F. S. Chakar and A. J. Ragauskas, Review of current and future softwood kraft lignin process chemistry, *Ind. Crops Prod.*, 2004, **20**, 131–141.
216 B. Joffres, D. Laurenti, N. Charon, A. Daudin, A. Quignard and C. Geantet, Thermochemical Conversion of Lignin for Fuels and Chemicals: A Review, *Oil Gas Sci. Technol.*, 2013, **68**, 753–763.
217 P. Azadi, O. R. Inderwildi, R. Farnood and D. A. King, Liquid fuels, hydrogen and chemicals from lignin: A critical review, *Renewable Sustainable Energy Rev.*, 2013, **21**, 506–523.
218 M. R. Sturgeon, M. H. O'Brien, P. N. Ciesielski, R. Katahira, J. S. Kruger, S. C. Chmely, J. Hamlin, K. Lawrence, G. B. Hunsinger, T. D. Foust, R. M. Baldwin, M. J. Biddy and G. T. Beckham, Lignin depolymerisation by nickel supported layered-double hydroxide catalysts, *Green Chem.*, 2014, **16**, 824–835.
219 G. T. Beckham, M. J. Biddy, S. C. Chmely and M. Sturgeon, Hydroxide catalysts for lignin depolymerization, US 20140107381 A1, 2014.
220 J. S. Kruger, N. S. Cleveland, S. T. Zhang, R. Katahira, B. A. Black, G. M. Chupka, T. Lammens, P. G. Hamilton, M. J. Biddy and G. T. Beckham, Lignin Depolymerization with Nitrate-Intercalated Hydrotalcite Catalysts, *ACS Catal.*, 2016, **6**, 1316–1328.
221 J. Mottweiler, M. Puche, C. Rauber, T. Schmidt, P. Concepcion, A. Corma and C. Bolm, Copper- and Vanadium-Catalyzed Oxidative Cleavage of Lignin using Dioxygen, *ChemSusChem*, 2015, **8**, 2106–2113.
222 K. Barta, T. D. Matson, M. L. Fettig, S. L. Scott, A. V. Iretskii and P. C. Ford, Catalytic disassembly of an organosolv lignin *via* hydrogen transfer from supercritical methanol, *Green Chem.*, 2010, **12**, 1640–1647.
223 K. Barta, G. R. Warner, E. S. Beach and P. T. Anastas, Depolymerization of organosolv lignin to aromatic compounds over Cu-doped porous metal oxides, *Green Chem.*, 2014, **16**, 191–196.
224 X. M. Huang, T. I. Koranyi, M. D. Boot and E. J. M. Hensen, Catalytic Depolymerization of Lignin in Supercritical Ethanol, *ChemSusChem*, 2014, **7**, 2276–2288.
225 X. M. Huang, C. Atay, T. I. Koranyi, M. D. Boot and E. J. M. Hensen, Role of Cu-Mg-Al Mixed Oxide Catalysts in Lignin Depolymerization in Supercritical Ethanol, *ACS Catal.*, 2015, **5**, 7359–7370.
226 X. M. Huang, T. I. Koranyi, M. D. Boot and E. J. M. Hensen, Ethanol as capping agent and formaldehyde scavenger for efficient depolymerization of lignin to aromatics, *Green Chem.*, 2015, **17**, 4941–4950.
227 D. D. Laskar, B. Yang, H. Wang and J. Lee, Pathways for biomass-derived lignin to hydrocarbon fuels, *Biofuels, Bioprod. Biorefin.*, 2013, **7**, 602–626.
228 M. Saidi, F. Samimi, D. Karimipourfard, T. Nimmanwudipong, B. C. Gates and M. R. Rahimpour, Upgrading of lignin-derived bio-oils by catalytic hydrodeoxygenation, *Energy Environ. Sci.*, 2014, **7**, 103–129.
229 J. Y. Shen, B. Guang, M. Tu and Y. Chen, Preparation and characterization of Fe/MgO catalysts obtained from hydrotalcite-like compounds, *Catal. Today*, 1996, **30**, 77–82.
230 A. A. Khassin, T. M. Yurieva, G. N. Kustova, I. S. Itenberg, M. P. Demeshkina, T. A. Krieger, L. M. Plyasova,

G. K. Chermashentseva and V. N. Parmon, Cobalt-aluminum co-precipitated catalysts and their performance in the Fischer-Tropsch synthesis, *J. Mol. Catal. A: Chem.*, 2001, **168**, 193–207.

231 A. Di Fronzo, C. Pirola, A. Comazzi, F. Galli, C. L. Bianchi, A. Di Michele, R. Vivani, M. Nocchetti, M. Bastianini and D. C. Boffito, Co-based hydrotalcites as new catalysts for the Fischer–Tropsch synthesis process, *Fuel*, 2014, **119**, 62–69.

232 A. Forgionny, J. L. G. Fierro, F. Mondragón and A. Moreno, Effect of Mg/Al Ratio on Catalytic Behavior of Fischer–Tropsch Cobalt-Based Catalysts Obtained from Hydrotalcites Precursors, *Top. Catal.*, 2016, **59**, 230–240.

233 P. Azadi, O. R. Inderwildi, R. Farnood and D. A. King, Liquid fuels, hydrogen and chemicals from lignin: A critical review, *Renewable Sustainable Energy Rev.*, 2013, **21**, 506–523.

234 A. M. Ribeiro, J. C. Santos and A. E. Rodrigues, PSA design for stoichiometric adjustment of bio-syngas for methanol production and co-capture of carbon dioxide, *Chem. Eng. J.*, 2010, **163**, 355–363.

235 S. R. Wang, H. X. Wang, Q. Q. Yin, L. J. Zhu and S. Yin, Methanation of bio-syngas over a biochar supported catalyst, *New J. Chem.*, 2014, **38**, 4471–4477.

236 T. Hanaoka, S. Inoue, S. Uno, T. Ogi and T. Minowa, Effect of woody biomass components on air-steam gasification, *Biomass Bioenergy*, 2005, **28**, 69–76.

237 I. Czekaj, F. Loviat, F. Raimondi, J. Wambach, S. Biollaz and A. Wokaun, Characterization of surface processes at the Ni-based catalyst during the methanation of biomass-derived synthesis gas: X-ray photoelectron spectroscopy (XPS), *Appl. Catal., A*, 2007, **329**, 68–78.

238 T. M. Roberge, S. O. Blavo, C. Holt, P. H. Matter and J. N. Kuhn, Effect of Molybdenum on the Sulfur-Tolerance of Cerium-Cobalt Mixed Oxide Water-Gas Shift Catalysts, *Top. Catal.*, 2013, **56**, 1892–1898.

239 C. Li and K. Suzuki, Tar property, analysis, reforming mechanism and model for biomass gasification—An overview, *Renewable Sustainable Energy Rev.*, 2009, **13**, 594–604.

240 O. Faix and D. Meier, Pyrolytic and hydrogenolytic degradation studies on lignocellulosics, pulps and lignins, *Holz Roh- Werkst.*, 1989, **47**, 67–72.

241 V. Pasangulapati, K. D. Ramachandriya, A. Kumar, M. R. Wilkins, C. L. Jones and R. L. Huhnke, Effects of cellulose, hemicellulose and lignin on thermochemical conversion characteristics of the selected biomass, *Bioresour. Technol.*, 2012, **114**, 663–669.

242 C. Font Palma, Modelling of tar formation and evolution for biomass gasification: A review, *Appl. Energy*, 2013, **111**, 129–141.

243 H. Yu, Z. Zhang, Z. Li and D. Chen, Characteristics of tar formation during cellulose, hemicellulose and lignin gasification, *Fuel*, 2014, **118**, 250–256.

244 K. Qian and A. Kumar, Reforming of lignin-derived tars over char-based catalyst using Py-GC/MS, *Fuel*, 2015, **162**, 47–54.

245 G. Guan, M. Kaewpanha, X. Hao and A. Abudula, Catalytic steam reforming of biomass tar: Prospects and challenges, *Renewable Sustainable Energy Rev.*, 2016, **58**, 450–461.

246 D. Li, M. Tamura, Y. Nakagawa and K. Tomishige, Metal catalysts for steam reforming of tar derived from the gasification of lignocellulosic biomass, *Bioresour. Technol.*, 2015, **178**, 53–64.

247 Y. Shen and K. Yoshikawa, Recent progresses in catalytic tar elimination during biomass gasification or pyrolysis—A review, *Renewable Sustainable Energy Rev.*, 2013, **21**, 371–392.

248 H. Watanabe, D. Li, Y. Nakagawa, K. Tomishige and M. M. Watanabe, Catalytic gasification of oil-extracted residue biomass of Botryococcus braunii, *Bioresour. Technol.*, 2015, **191**, 452–459.

249 D. Li, L. Wang, M. Koike, Y. Nakagawa and K. Tomishige, Steam reforming of tar from pyrolysis of biomass over Ni/Mg/Al catalysts prepared from hydrotalcite-like precursors, *Appl. Catal., B*, 2011, **102**, 528–538.

250 M. Koike, D. Li, Y. Nakagawa and K. Tomishige, A Highly Active and Coke-Resistant Steam Reforming Catalyst Comprising Uniform Nickel–Iron Alloy Nanoparticles, *ChemSusChem*, 2012, **5**, 2312–2314.

251 D. Li, M. Koike, L. Wang, Y. Nakagawa, Y. Xu and K. Tomishige, Regenerability of Hydrotalcite-Derived Nickel–Iron Alloy Nanoparticles for Syngas Production from Biomass Tar, *ChemSusChem*, 2014, **7**, 510–522.

252 M. Koike, D. Li, H. Watanabe, Y. Nakagawa and K. Tomishige, Comparative study on steam reforming of model aromatic compounds of biomass tar over Ni and Ni–Fe alloy nanoparticles, *Appl. Catal., A*, 2015, **506**, 151–162.

253 L. Wang, D. Li, H. Watanabe, M. Tamura, Y. Nakagawa and K. Tomishige, Catalytic performance and characterization of Co/Mg/Al catalysts prepared from hydrotalcite-like precursors for the steam gasification of biomass, *Appl. Catal., B*, 2014, **150–151**, 82–92.

254 L. Wang, J. Chen, H. Watanabe, Y. Xu, M. Tamura, Y. Nakagawa and K. Tomishige, Catalytic performance and characterization of Co–Fe bcc alloy nanoparticles prepared from hydrotalcite-like precursors in the steam gasification of biomass-derived tar, *Appl. Catal., B*, 2014, **160–161**, 701–715.

255 D. Li, M. Koike, J. Chen, Y. Nakagawa and K. Tomishige, Preparation of Ni–Cu/Mg/Al catalysts from hydrotalcite-like compounds for hydrogen production by steam reforming of biomass tar, *Int. J. Hydrogen Energy*, 2014, **39**, 10959–10970.

256 D. Li, M. Lu, K. Aragaki, M. Koike, Y. Nakagawa and K. Tomishige, Characterization and catalytic performance of hydrotalcite-derived Ni-Cu alloy nanoparticles catalysts

for steam reforming of 1-methylnaphthalene, *Appl. Catal., B*, 2016, **192**, 171–181.
257 J. Chen, M. Tamura, Y. Nakagawa, K. Okumura and K. Tomishige, Promoting effect of trace Pd on hydrotalcite-derived Ni/Mg/Al catalyst in oxidative steam reforming of biomass tar, *Appl. Catal., B*, 2015, **179**, 412–421.
258 E. Furimsky, Catalytic hydrodeoxygenation, *Appl. Catal., A*, 2000, **199**, 147–190.
259 D. Delledonne, D. Bianchi and R. Buzzoni, Catalysts and process for the liquefaction of lignins, EP 2483330 A1, 2012.
260 G.-Y. Xu, J.-H. Guo, Y.-C. Qu, Y. Zhang, Y. Fu and Q.-X. Guo, Selective hydrodeoxygenation of lignin-derived phenols to alkyl cyclohexanols over a Ru-solid base bifunctional catalyst, *Green Chem.*, 2016, **18**, 5510–5517.
261 O. Vozniuk, S. Agnoli, L. Artiglia, A. Vassoi, N. Tanchoux, F. Di Renzo, G. Granozzi and F. Cavani, Towards an improved process for hydrogen production: the chemical-loop reforming of ethanol, *Green Chem.*, 2016, **18**, 1038–1050.
262 R. Torralba-Sánchez, D. López-Jurado, J. A. Rivera, G. Fetter, R. Hernández-Huesca, M. A. Pérez-Cruz and P. Bosch, High-Performance Materials Based on Lithium-Containing Hydrotalcite-Bayerite Composites for Biogas Upgrade, *Energy Fuels*, 2016, **30**, 7474–7480.
263 A. Fahami, F. S. Al-Hazmi, A. A. Al-Ghamdi, W. E. Mahmoud and G. W. Beall, Structural characterization of chlorine intercalated Mg-Al layered double hydroxides: A comparative study between mechanochemistry and hydrothermal methods, *J. Alloys Compd.*, 2016, **683**, 100–107.

